THE EUROPEAN
PHYSICAL JOURNAL C

Search for new physics in top quark production in dilepton final states in proton-proton collisions at $\sqrt{s} = 13\,\text{TeV}$

CMS Collaboration[*]

CERN

Abstract A search for new physics in top quark production is performed in proton-proton collisions at 13 TeV. The data set corresponds to an integrated luminosity of $35.9\,\text{fb}^{-1}$ collected in 2016 with the CMS detector. Events with two opposite-sign isolated leptons (electrons or muons), and b quark jets in the final state are selected. The search is sensitive to new physics in top quark pair production and in single top quark production in association with a W boson. No significant deviation from the standard model expectation is observed. Results are interpreted in the framework of effective field theory and constraints on the relevant effective couplings are set, one at a time, using a dedicated multivariate analysis. This analysis differs from previous searches for new physics in the top quark sector by explicitly separating tW from $\text{t}\bar{\text{t}}$ events and exploiting the specific sensitivity of the tW process to new physics.

1 Introduction

Because of its large mass, close to the electroweak (EW) symmetry breaking scale, the top quark is predicted to play an important role in several new physics scenarios. If the new physics scale is in the available energy range of the CERN LHC, the existence of new physics could be directly observed via the production of new particles. Otherwise, new physics could affect standard model (SM) interactions indirectly, through modifications of SM couplings or enhancements of rare SM processes. In this case, it is useful to introduce a model independent approach to parametrize and constrain possible deviations from SM predictions, independently of the fundamental theory of new physics.

Several searches for new physics in the top quark sector including new non-SM couplings of the top quark have been performed at the Tevatron and LHC colliders [1–4,4–10]. Most of the previous analyses followed the anomalous coupling approach in which the SM Lagrangian is extended for possible new interactions. Another powerful framework

to parametrize deviations with respect to the SM prediction is the effective field theory (EFT) [11,12]. Constraints obtained on anomalous couplings can be translated to the effective coupling bounds [1,13]. Several groups have performed global fits of top quark EFT to unfolded experimental data from the Tevatron and LHC colliders [14,15]. Due to the limited access to data and details of the associated uncertainties, correlations between various cross section measurements and related uncertainties are neglected in a global fit on various unfolded measurements. On the other hand, EFT operators could affect backgrounds for some processes constructively or destructively while cross sections are measured with the SM assumptions for background processes. Inside the CMS Collaboration and with direct access to data, all mentioned points could be considered properly.

In this paper, the EFT approach is followed to search for new physics in the top quark sector in the dilepton final states. In Refs. [13,16], all dimension-six operators that contribute to top quark pair ($\text{t}\bar{\text{t}}$) production and single top quark production in association with a W boson (tW) are investigated. The operators and the related effective Lagrangians, which are relevant for dilepton final states, can be written as [12]:

$$O_{\phi\text{q}}^{(3)} = (\phi^+ \tau^i D_\mu \phi)(\bar{\text{q}}\gamma^\mu \tau^i \text{q}),$$

$$L_{\text{eff}} = \frac{C_{\phi\text{q}}^{(3)}}{\sqrt{2}\Lambda^2} g v^2 \bar{\text{b}}\gamma^\mu P_{\text{L}} \text{t} W_\mu^- + \text{h.c.}, \tag{1}$$

$$O_{\text{tW}} = (\bar{\text{q}}\sigma^{\mu\nu}\tau^i \text{t})\tilde{\phi} W_{\mu\nu}^i,$$

$$L_{\text{eff}} = -2\frac{C_{\text{tW}}}{\Lambda^2} v \bar{\text{b}}\sigma^{\mu\nu} P_{\text{R}} \text{t} \partial_\nu W_\mu^- + \text{h.c.}, \tag{2}$$

$$O_{\text{tG}} = (\bar{\text{q}}\sigma^{\mu\nu}\lambda^a \text{t})\tilde{\phi} G_{\mu\nu}^a,$$

$$L_{\text{eff}} = \frac{C_{\text{tG}}}{\sqrt{2}\Lambda^2} v \left(\bar{\text{t}}\sigma^{\mu\nu}\lambda^a \text{t}\right) G_{\mu\nu}^a + \text{h.c.}, \tag{3}$$

$$O_{\text{G}} = f_{abc} G_\mu^{a\nu} G_\nu^{b\rho} G_\rho^{c\mu},$$

$$L_{\text{eff}} = \frac{C_{\text{G}}}{\Lambda^2} f_{abc} G_\mu^{a\nu} G_\nu^{b\rho} G_\rho^{c\mu}, \tag{4}$$

$$O_{\text{u(c)G}} = (\bar{\text{q}}\sigma^{\mu\nu}\lambda^a \text{t})\tilde{\phi} G_{\mu\nu}^a,$$

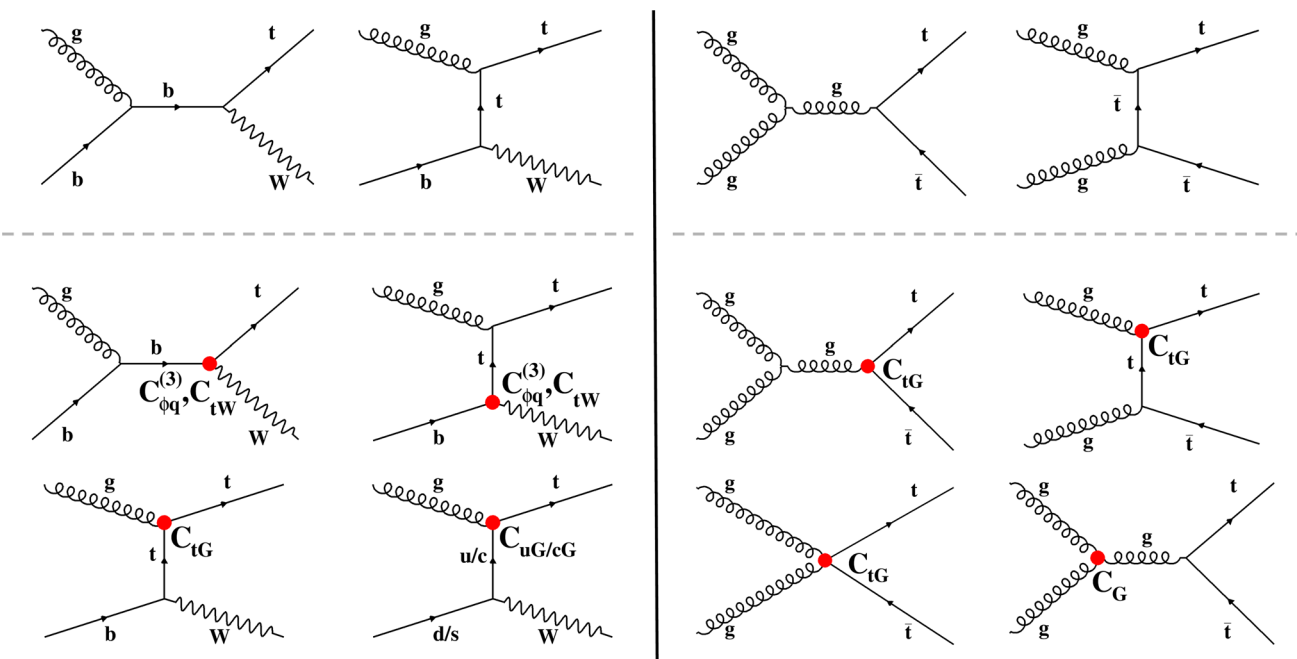[*] e-mail: cms-publication-committee-chair@cern.ch

Springer

Fig. 1 Representative Feynman diagrams for the tW (left panel) and $t\bar{t}$ (right panel) production at leading order. The upper row presents the SM diagrams, the middle and lower rows present diagrams corresponding to the $O_{\phi q}^{(3)}$, O_{tW}, O_{tG}, O_G and $O_{u/cG}$ contributions

$$L_{\text{eff}} = \frac{C_{\text{u(c)G}}}{\sqrt{2}\Lambda^2} v \left(\bar{u}\,(\bar{c})\,\sigma^{\mu\nu}\lambda^a t\right) G_{\mu\nu}^a + \text{h.c.}, \tag{5}$$

where $D_\mu = \partial_\mu - i g_s \frac{1}{2}\lambda^a G_\mu^a - i g \frac{1}{2}\tau^i W_\mu^i - i g' Y B_\mu$, $W_{\mu\nu}^i = \partial_\mu W_\nu^i - \partial_\nu W_\mu^i + g\epsilon_{ijk} W_\mu^j W_\nu^k$, $G_{\mu\nu}^a = \partial_\mu G_\nu^a - \partial_\nu G_\mu^a + g_s f^{abc} G_\mu^b G_\nu^c$, $\sigma^{\mu\nu} = \frac{1}{2}[\gamma^\mu, \gamma^\nu]$, $P_{\text{L,R}} = \frac{1}{2}(1 \mp \gamma^5)$, and the symbols q, t and ϕ ($\tilde{\phi} = \epsilon\phi^*$) in the operators represent the left-handed quark doublet, the right-handed top quark singlet, and the Higgs boson doublet fields, respectively. The parameters $C_{\phi q}^{(3)}$, C_{tW}, C_{tG}, C_G and $C_{\text{u(c)G}}$ stand for the dimensionless Wilson coefficients, also called effective couplings. The variable Λ represents the energy scale beyond which new physics becomes relevant. A detailed description of the operators is given in Refs. [13,16,17]. In this analysis, four-fermion operators involved in $t\bar{t}$ production are not probed. Up to order Λ^{-2}, the tW and $t\bar{t}$ production cross sections and most of the differential observables considered in this analysis do not receive CP-odd contributions. Therefore, we only probe CP-even operators with real coefficients. The operators $O_{\phi q}^{(3)}$ and O_{tW} modify the SM interaction between the W boson, top quark, and b quark (Wtb). We consider the EFT effects in the production of top quarks not in their decays [18]. The operator O_{tG} is called the chromomagnetic dipole moment operator of the top quark and can arise from various models of new physics [19,20]. The triple-gluon field strength operator O_G represents the only genuinely gluonic CP conserving term that can appear at dimension six within an effective strong interaction Lagrangian. Although it is

shown that jet production at the LHC can set a tight constraint on the C_G [21], $t\bar{t}$ production is also considered as a promising channel [22,23]. The operators O_{uG} and O_{cG} lead to flavor-changing neutral current (FCNC) interactions of the top quark and contribute to tW production. The effect of introducing new couplings $C_{\phi q}^{(3)}$, C_{tW}, C_{tG} and $C_{u(c)G}$ can be investigated in tW production. The chromomagnetic dipole moment operator of the top quark also affects $t\bar{t}$ production. In the case of C_G coupling, only $t\bar{t}$ production is modified. It should be noted that the O_{tW} and O_{tG} operators with imaginary coefficients lead to CP-violating effects. Representative Feynman diagrams for SM and new physics contributions in tW and $t\bar{t}$ production are shown in Fig. 1.

A variety of limits have been set on the Wtb anomalous coupling through single top quark t-channel production and measurements of the W boson polarization from top quark decay by the D0 [1], ATLAS [2,3] and CMS [4,5] Collaborations. Direct limits on the top quark chromomagnetic dipole moment have been obtained by the CMS Collaboration at 7 and 13 TeV using top quark pair production events [6,10]. Searches for top quark FCNC interactions have been performed at the Tevatron [7,8] and LHC [4,9] via single top quark production and limits are set on related anomalous couplings.

In this paper, a search for new physics in top quark production using an EFT framework is reported. This is the first such search for new physics that uses the tW process. Final states with two opposite-sign isolated leptons (electrons or muons) in association with jets identified as originating from

the fragmentation of a bottom quark ("bjets") are analyzed. The search is sensitive to new physics contributions to tW and $t\bar{t}$ production, and the six effective couplings, C_G, $C_{\phi q}^{(3)}$, C_{tW}, C_{tG}, C_{uG}, and C_{cG}, are constrained assuming one non-zero effective coupling at a time. The effective couplings affect both the rate of $t\bar{t}$ and tW production and the kinematic distributions of final state particles. For the $C_{\phi q}^{(3)}$, C_{tW}, C_{tG}, and C_G effective couplings, the deviation from the SM prediction is dominated by the interference term between SM and new physics diagrams, which is linear with respect to the effective coupling. Therefore, the kinematic distributions of the final-state particles vary as a function of the Wilson coefficients. For small effective couplings the kinematic distributions approach those predicted by the SM. On the other hand, the new physics terms due to the C_{uG} and C_{cG} effective couplings do not interfere with the SM tW process, and the kinematic distributions of final-state particles are determined by the new physics terms independently of the SM prediction. In this analysis, we use the rates of tW and $t\bar{t}$ production to probe the $C_{\phi q}^{(3)}$, C_{tW}, C_{tG}, and C_G effective couplings. Variations in both rate and kinematic distributions of final-state particles are employed to probe the C_{uG} and C_{cG} effective couplings. The analysis utilizes proton-proton (pp) collision data collected by the CMS experiment in 2016 at a center-of-mass energy of 13 TeV, corresponding to an integrated luminosity of 35.9 fb^{-1}.

The paper is structured as follows. In Sect. 2, a description of the CMS detector is given and the simulated samples used in the analysis are detailed. The event selection and the SM background estimation are presented in Sect. 3. Section 4 presents a description of the signal extraction procedure. An overview of the systematic uncertainty treatment is given in Sect. 5. Finally, the constraints on the effective couplings are presented in Sect. 6, and a summary is given in Sect. 7.

2 The CMS detector and event simulation

The central feature of the CMS apparatus is a superconducting solenoid of 6 m internal diameter, providing a magnetic field of 3.8 T. Within the solenoid volume are a silicon pixel and strip tracker, a lead tungstate crystal electromagnetic calorimeter (ECAL), and a brass and scintillator hadron calorimeter, each composed of a barrel and two endcap sections. Forward calorimeters extend the pseudorapidity (η) coverage provided by the barrel and endcap detectors. Muons are detected in gas-ionisation chambers embedded in the steel flux-return yoke outside the solenoid. A more detailed description of the CMS detector, together with a definition of the coordinate system used and the relevant kinematic variables, can be found in Ref. [24].

The Monte Carlo (MC) samples for the $t\bar{t}$, tW and diboson (VV = WW, WZ, ZZ) SM processes are simulated using the POWHEG- BOX event generator (v1 for tW, v2 for $t\bar{t}$ and diboson) [25–28] at the next-to-leading order (NLO), interfaced with PYTHIA (v8.205) [29] to simulate parton showering and to match soft radiations with the contributions from the matrix elements. The PYTHIA tune CUETP8M1 [30] is used for all samples except for the $t\bar{t}$ sample, for which the tune CUETP8M2 [31] is used. The NNPDF3.0 [32] set of the parton distribution functions (PDFs) is used. The $t\bar{t}$ and tW samples are normalized to the next-to-next-to-leading order (NNLO) and approximate NNLO cross section calculations, respectively [33,34]. In order to better describe the transverse momentum (p_T) distribution of the top quark in $t\bar{t}$ events, the top quark p_T spectrum simulated with POWHEG is reweighted to match the differential top quark p_T distribution at NNLO quantum chromoDynamics (QCD) accuracy and including EW corrections calculated in Ref. [35]. Other SM background contributions, from Drell–Yan (DY), $t\bar{t}$+V, $t\bar{t}$+γ, and W + γ processes, are simulated at NLO using the MADGRAPH5_aMC@NLO (v2.2.2) event generator [36–38], interfaced with PYTHIA v8 for parton showering and hadronization. The events include the effects of additional pp interactions in the same or nearby bunch crossings (pileup) and are weighted according to the observed pileup distribution in the analyzed data. The CMS detector response is simulated using GEANT4 (v9.4) [39,40], followed by a detailed trigger simulation. Simulated events are reconstructed with the same algorithms as used for data.

In order to calculate the total cross sections for the $t\bar{t}$ and tW processes and generate events in the presence of new effective interactions, the operators of Eqs. 1–5 have been implemented in the universal FEYNRULES output (UFO) format [41] through the FEYNRULES package [42]. The output EFT model is used in the MADGRAPH5_aMC@NLO (v2.2.2) event generator [36,37]. If we allow for the presence of one operator at a time, the total cross section up to $\mathcal{O}(\Lambda^{-4})$ can be parametrized as

$$\sigma = \sigma_{SM} + C_i \sigma_i^{(1)} + C_i^2 \sigma_i^{(2)}, \tag{6}$$

where the C_is are effective couplings introduced in Eqs. 1–5. Here, $\sigma_i^{(1)}$ is the contribution to the cross section due to the interference term between the SM diagrams and diagrams with one EFT vertex. The cross section $\sigma_i^{(2)}$ is the pure new physics contribution. We use the most precise available SM cross section prediction, which are $\sigma_{SM}^{t\bar{t}} = 832_{-29}^{+20}$ (scales) ± 35 (PDF + α_S) pb and $\sigma_{SM}^{tW} = 71.7 \pm 1.8$ (scales) ± 3.4 (PDF + α_S) pb for $t\bar{t}$ and tW production, respectively [33,34], where the α_S is strong coupling constant. The first uncertainty reflects the uncertainties in the factorization and renormalization scales. In the framework of EFT, the $\sigma_i^{(1)}$ and $\sigma_i^{(2)}$ terms have been calculated at NLO accuracy for all of the operators, except O_G [16,43,44]. At the time the work for this paper was concluded, there was no

Table 1 Contribution to the cross section due to the interference between the SM diagrams and diagrams with one EFT vertex ($\sigma_i^{(1)}$), and the pure new physics ($\sigma_i^{(2)}$) for $t\bar{t}$ and tW production [in pb] for the various effective couplings for $\Lambda = 1$ TeV. The respective K factors ($\sigma_i^{\mathrm{NLO}}/\sigma_i^{\mathrm{LO}}$) are also shown

Channel	Contribution	C_G	$C_{\phi\mathrm{q}}^{(3)}$	C_tW	C_tG	C_uG	C_cG
$t\bar{t}$	$\sigma_i^{(1)-\mathrm{LO}}$	31.9 pb	–	–	137 pb	–	–
	$K^{(1)}$	–	–	–	1.48	–	–
	$\sigma_i^{(2)-\mathrm{LO}}$	102.3 pb	–	–	16.4 pb	–	–
	$K^{(2)}$	–	–	–	1.44	–	–
t W	$\sigma_i^{(1)-\mathrm{LO}}$	–	6.7 pb	−4.5 pb	3.3 pb	0	0
	$K^{(1)}$	–	1.32	1.27	1.27	0	0
	$\sigma_i^{(2)-\mathrm{LO}}$	–	0.2 pb	1 pb	1.2 pb	16.2 pb	4.6 pb
	$K^{(2)}$	–	1.31	1.18	1.06	1.27	1.27

available UFO model including the O_G operator at the NLO. The values of $\sigma_i^{(1)}$ and $\sigma_i^{(2)}$ for various effective couplings at LO and available K factors are given in Table 1.

3 Event selection and background estimation

The event selection for this analysis is similar to the one used in Ref. [10]. The events of interest are recorded by the CMS detector using a combination of dilepton and single-lepton triggers. Single-lepton triggers require at least one isolated electron (muon) with $p_\mathrm{T} > 27\,(24)$ GeV. The dilepton triggers select events with at least two leptons with loose isolation requirements and p_T for the leading and sub-leading leptons greater than 23 and 12 (17 and 8) GeV for the ee ($\mu\mu$) final state. In the eμ final state, in the case of the leading lepton being an electron, the events are triggered if the electron-muon pair has a p_T greater than 23 and 8 GeV for the electron and muon, respectively. In the case of the leading lepton being a muon, the trigger thresholds are 23 and 12 GeV for the muon and electron, respectively [45].

Offline, the particle-flow (PF) algorithm [46] aims to reconstruct and identify each individual particle with an optimized combination of information from the various elements of the CMS detector. Electron candidates are reconstructed using tracking and ECAL information [47]. Requirements on electron identification variables based on shower shape and track-cluster matching are further applied to the reconstructed electron candidates, together with isolation criteria [10,47]. Electron candidates are selected with $p_\mathrm{T} > 20$ GeV and $|\eta| < 2.4$. Electron candidates within the range $1.444 < |\eta| < 1.566$, which corresponds to the transition region between the barrel and endcap regions of the ECAL, are not considered. Information from the tracker and the muon spectrometer are combined in a global fit to reconstruct muon candidates [48]. Muon candidates are further required to have a high-quality fit including a minimum number of hits in both systems, and to be isolated [10,48]. The muons used in this analysis are selected inside the fiducial region of the muon spectrometer, $|\eta| < 2.4$, with a minimum p_T of 20 GeV.

The PF candidates are clustered into jets using the anti-k_T algorithm with a distance parameter of 0.4 [49–51]. Jets are calibrated in data and simulation, accounting for energy deposits of particles from pileup [52]. Jets with $p_\mathrm{T} > 30$ GeV and $|\eta| < 2.4$ are selected; loose jets are defined as jets with the p_T range between 20 and 30 GeV. Jets originating from the hadronization of b quarks are identified using the combined secondary vertex algorithm [53]; this algorithm combines information from track impact parameters and secondary vertices identified within a given jet. The chosen working point provides a signal identification efficiency of approximately 68% with a probability to misidentify light-flavor jets as bjets of approximately 1% [53]. The missing transverse momentum vector $\vec{p}_\mathrm{T}^{\,\mathrm{miss}}$ is defined as the projection on the plane perpendicular to the proton beams axis of the negative vector sum of the momenta of all reconstructed PF candidates in the event [54]. Corrections to the jet energies are propagated to $\vec{p}_\mathrm{T}^{\,\mathrm{miss}}$. Its magnitude is referred to as $p_\mathrm{T}^{\mathrm{miss}}$.

Events are required to have at least two leptons (electrons or muons) with opposite sign and with an invariant mass above 20 GeV. The leading lepton must fulfill $p_\mathrm{T} > 25$ GeV. For the same-flavor lepton channels, to suppress the DY background, the dilepton invariant mass must not be within 15 GeV of the Z boson mass and a minimal value (of 60 GeV) on $p_\mathrm{T}^{\mathrm{miss}}$ is applied.

The events are divided into the ee, eμ, and $\mu\mu$ channels according to the flavors of the two leptons with the highest p_T and are further categorized in different bins depending on the number of jets ("n-jets") and number b-tagged jets ("m-tags") in the final state. The largest number of tW events is expected in the category with exactly one b-tagged jet (1-jet,1-tag) followed by the category with two jets, of which one a bjet (2-jets,1-tag). Events in the categories with more than two jets and exactly two b-tagged jets are dominated by the $t\bar{t}$ process ($\geq$2-jets,2-tags). Categories with zero bjets are dominated by DY events in the ee and $\mu\mu$ channels and
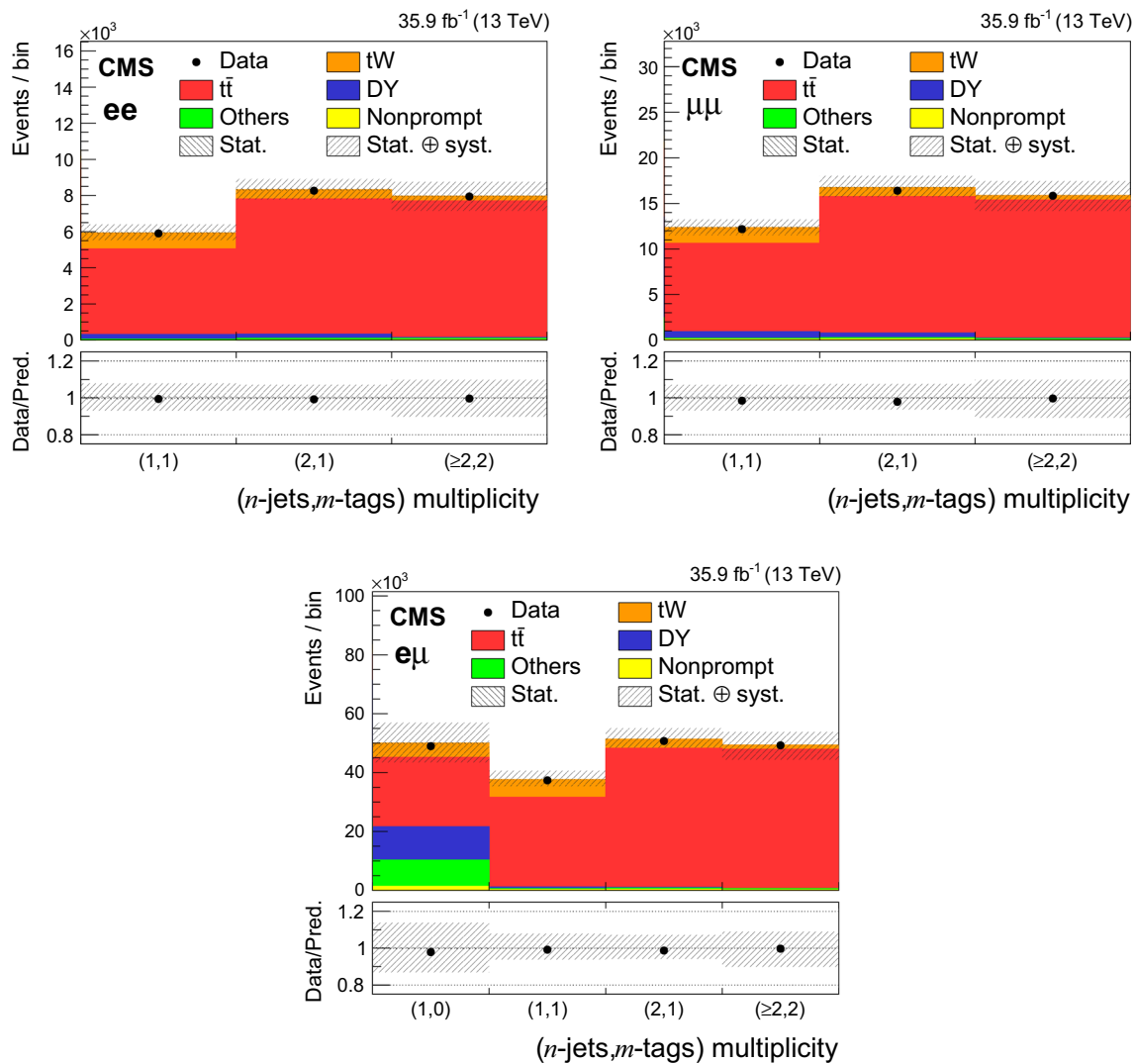
Fig. 2 The observed number of events and SM background predictions in the search regions of the analysis for the ee (upper left), $\mu\mu$ (upper right), and eμ (lower) channels. The hatched bands correspond to the quadratic sum of statistical and systematic uncertainties in the event yield for the SM background predictions. The ratios of data to the sum of the predicted yields are shown at the bottom of each plot. The narrow hatched bands represent the contribution from the statistical uncertainty in the MC simulation

are not used in the analysis. However, in the eμ channel, the contamination of DY events is lower and a significant number of tW events is present in the category with one jet and zero b-tagged jets (1-jet,0-tag). The latter category is included in this analysis. In Fig. 2, the data in the ten search regions are shown together with the SM background predictions.

The contributions of SM processes leading to two prompt leptons in the final state are estimated from simulated samples and are normalised to the integrated luminosity of the data. These contributions originate mainly from $t\bar{t}$, tW and DY production. Other SM processes, such as diboson, $t\bar{t}$+V and $t\bar{t}+\gamma$ have significantly smaller contributions.

To correct the DY simulation for the efficiency of the p_T^{miss} threshold and for the mismodeling of the heavy-flavour con-

tent, scale factors are derived using the ratio of the numbers of simulated events inside and outside the dilepton invariant mass window, 76–106 GeV. The observed event yield inside the window is scaled to estimate the DY background outside the mass window [55].

The nonprompt lepton backgrounds which contain fake lepton(s) from a misreconstructed γ or jet(s) are also considered. The contribution of misidentified or converted γ events from the Wγ process is estimated from MC simulation. The contribution from W+jets and multijet processes is estimated by a data-based technique using events with same-sign leptons. The method is based on the assumption that the probability of assigning positive or negative charge to the fake lepton is equal. Therefore, the background contribution from

Table 2 Number of expected events from tW, t$\bar{\text{t}}$ and DY production, from the remaining backgrounds (other), total background contribution and observed events in data after all selections for the ee, eμ, and μμ channels and for different (*n*-jets,*m*-tags) categories. The uncer-tainties correspond to the statistical contribution only for the individual background predictions and to the quadratic sum of the statistical and systematic contributions for the total background predictions

Channel	(*n*-jets,*m*-tags)	Prediction					Data
		t W	t$\bar{\text{t}}$	DY	Other	Total yield	
ee	(1,1)	884 ± 8	4741 ± 15	258 ± 50	53 ± 5	5936 ± 470	5902
	(2,1)	518 ± 6	7479 ± 19	241 ± 53	94 ± 5	8331 ± 597	8266
	($\geq$2,2)	267 ± 4	7561 ± 18	46 ± 24	99 ± 4	7973 ± 819	7945
eμ	(1,0)	4835 ± 20	23557 ± 35	11352 ± 277	10294 ± 72	50038 ± 6931	48973
	(1,1)	6048 ± 22	30436 ± 38	561 ± 66	629 ± 13	37673 ± 2984	37370
	(2,1)	3117 ± 16	47206 ± 48	278 ± 48	781 ± 9	51382 ± 3714	50725
	($\geq$2,2)	1450 ± 10	47310 ± 46	32 ± 22	598 ± 9	49391 ± 5010	49262
μμ	(1,1)	1738 ± 12	9700 ± 21	744 ± 90	183 ± 5	12366 ± 879	12178
	(2,1)	989 ± 9	14987 ± 27	501 ± 75	275 ± 5	16751 ± 1276	16395
	($\geq$2,2)	508 ± 6	15136 ± 26	82 ± 24	163 ± 5	15889 ± 1714	15838

Table 3 Summary of the observables used to probe the effective couplings in various (*n*-jets,*m*-tags) categories in the ee, eμ, and μμ channels

Eff. coupling	Channel	Categories				
		1-jet, 0-tag	1-jet, 1-tag	2-jets, 1-tag	>2-jets, 1-tag	$\geq$2-jets, 2-tags
C_G	ee	–	Yield	Yield	–	Yield
	eμ	Yield	Yield	Yield	–	Yield
	μμ	–	Yield	Yield	–	Yield
$C_{\phi q}^{(3)}$, C_{tW}, C_{tG}	ee	–	NN_{11}	NN_{21}	–	Yield
	eμ	NN_{10}	NN_{11}	NN_{21}	–	Yield
	μμ	–	NN_{11}	NN_{21}	–	Yield
C_{uG}, C_{cG}	ee	–	NN_{FCNC}			–
	eμ	–	NN_{FCNC}			–
	μμ	–	NN_{FCNC}			–

fake leptons in the final selection (opposite-sign sample) can be estimated from the corresponding sample with same-sign leptons. In this latter same-sign event sample, the remaining small contribution from prompt-lepton backgrounds is subtracted from data using MC samples.

After all selections, the expected numbers of events from tW, t$\bar{\text{t}}$, DY, and remaining background contributions mentioned above, as well as the total number of background events are reported in Table 2 for the ee, eμ, and μμ channels and for the various (*n*-jets,*m*-tags) categories. We find generally very good agreement between data and predictions, within the uncertainties of the data.

4 Signal extraction using neural networks tools

The purpose of the analysis is to search for deviations from the SM predictions in the tW and t$\bar{\text{t}}$ production due to new physics, parametrized with the presence of new effective cou-plings. In order to investigate the effect of the non-zero effective couplings, it is important to find suitable variables with high discrimination power between the signal and the background. Depending on the couplings, the total yield or the distribution of the output of a neural network (NN) algorithm is employed, as summarized in Table 3. The NN algorithm used in this analysis is a multilayer perceptron [56].

All the effective couplings introduced in Sect. 1 can contribute to tW production except the triple gluon field strength operator, O_G which only affects t$\bar{\text{t}}$ production. As observed in previous analysis [22] and confirmed here, the top quark p_T distribution is sensitive to the triple-gluon field-strength operator. The kinematic distributions of final-state particles show less discrimination power than the top quark p_T distribution. In addition, they vary with the value of C_G and approach the SM prediction for decreasing values of C_G. Therefore, we use the total yield in various categories to constrain the C_G effective coupling.

The deviation from the SM tW production because of the interference between the SM and the O_{tG}, $O_{\phi q}^{(3)}$, and O_{tW} operators is of the order of $1/\Lambda^2$. It is assumed that the new physics scale Λ is larger than the scale we probe. Therefore, $1/\Lambda^4$ contributions from the new physics terms are small compared to the contribution from the interference term. The operator $O_{\phi q}^{(3)}$ is similar to the SM Wtb operator and leads to a rescaling of the SM Wtb vertex [13]. The O_{tW} and O_{tG} operators lead to the right-handed Wtb interaction and a tensor-like ttg interaction, respectively, which are absent in the SM at the first order. Their effects have been investigated via the various kinematic distributions of the final-state particles considered in this analysis and are found to be not distinguishable from the SM tW and $t\bar{t}$ processes for unconstrained values of the effective couplings within the current precision on data. After the selection described in Section 3, the dominant background comes from $t\bar{t}$ production, with a contribution of about 90%. In order to observe deviations from SM tW production in the presence of the $O_{\phi q}^{(3)}$, O_{tW}, and O_{tG} effective operators, we need to separate tW events from the large number of $t\bar{t}$ events. Two independent NNs are trained to separate $t\bar{t}$ events (the background) and tW events (considered as the signal) in the (1-jet, 1-tag) (NN_{11}) and (2-jets, 1-tag) (NN_{21}) categories, which have significant signal contributions [57]. For the eμ channel, another NN is used for the (1-jet, 0-tag) (NN_{10}) category, in which the $t\bar{t}$, WW, and DY events are combined and are considered as the background. A comparison between the observed data and the SM background prediction of the NN output shape in various (n-jets, m-tags) categories is shown for the ee and $\mu\mu$ channels in Fig. 3 and for the eμ channel in Fig. 4 (left column).

The presence of the O_{uG} and O_{cG} operators changes the initial-state particle (see Fig. 1), and leads to different kinematic distributions for the final-state particles, compared to the SM tW process. For these FCNC operators, new physics effects on final-state particle distributions are expected to be distinguishable from SM processes. In order to search for new physics due to the O_{uG} and O_{cG} effective operators, an NN (NN_{FCNC}) is used to separate SM backgrounds ($t\bar{t}$ and tW events together) and new physics signals for events with exactly one b-tagged jet with no requirement on the number of light-flavor jets (n-jets, 1-tag). The comparison of the NN output for data, SM background and signal (tW events via FCNC interactions) is shown in Fig. 4 (right column) for the ee, eμ, and $\mu\mu$ channels.

The various input variables for training the NN introduced above are described below and are shown in Table 4.

- $M_{\ell\ell}$ (where ℓ = e or μ), invariant mass of dilepton system;
- $p_T^{\ell\ell}$, p_T of dilepton system;
- $\Delta p_T(\ell_1, \ell_2)$, $p_T^{\text{leading lepton}} - p_T^{\text{sub-leading lepton}}$;
- $p_T^{\ell_1}$, p_T of leading lepton;
- Centrality(ℓ_1, jet$_1$), scalar sum of p_T of the leading lepton and leading jet, over total energy of selected leptons and jets;
- Centrality(ℓ_1, ℓ_2), scalar sum of p_T of the leading and sub-leading leptons, over total energy of selected leptons and jets;
- $\Delta\Phi(\ell\ell$, jet$_1$), $\Delta\Phi$ between dilepton system and leading jet where Φ is azimuthal angle;
- p_T ($\ell\ell$, jet$_1$), p_T of dilepton and leading jet system;
- p_T (ℓ_1, jet$_1$), p_T of leading lepton and leading jet system;
- Centrality($\ell\ell$, jet$_1$), scalar sum of p_T of the dilepton system and leading jet, over total energy of selected leptons and jets;
- $\Delta R(\ell_1, \ell_2)$, $\sqrt{(\eta^{\ell_1} - \eta^{\ell_2})^2 + (\Phi^{\ell_1} - \Phi^{\ell_2})^2}$;
- $\Delta R(\ell_1$, jet$_1$), $\sqrt{(\eta^{\ell_1} - \eta^{\text{jet}_1})^2 + (\Phi^{\ell_1} - \Phi^{\text{jet}_1})^2}$;
- $M(\ell_1$, jet$_1$), invariant mass of leading lepton and leading jet;
- $M($jet$_1$, jet$_2$), invariant mass of leading jet and sub-leading jet;
- $\Delta R(\ell_1$, jet$_2$), $\sqrt{(\eta^{\ell_1} - \eta^{\text{jet}_2})^2 + (\Phi^{\ell_1} - \Phi^{\text{jet}_2})^2}$;
- $\Delta R(\ell\ell$, jet$_1$), $\sqrt{(\eta^{\ell\ell} - \eta^{\text{jet}_1})^2 + (\Phi^{\ell\ell} - \Phi^{\text{jet}_1})^2}$;
- $\Delta p_T(\ell_2$, jet$_2$), $p_T^{\ell_2} - p_T^{\text{jet}_2}$;
- $M(\ell_2$, jet$_1$), invariant mass of sub-leading lepton and leading jet.

5 Systematic uncertainties

The normalization and shape of the signal and the backgrounds are both affected by different sources of systematic uncertainty. For each source, an induced variation can be parametrized, and treated as a nuisance parameter in the fit that is described in the next section.

A systematic uncertainty of 2.5% is assigned to the integrated luminosity and is used for signal and background rates [58]. The efficiency corrections for trigger and offline selection of leptons were estimated by comparing the efficiency measured in data and in MC simulation using $Z \to \ell\ell$ events, based on a "tag-and-probe" method as in Ref. [59]. The scale factors obtained are varied by one standard deviation to take into account the corresponding uncertainties in the efficiency. The jet energy scale and resolution uncertainties depend on p_T and η of the jet and are computed by shifting the energy of each jet and propagating the variation to $\vec{p}_T^{\text{miss}}$ coherently [60].

The uncertainty in the b tagging is estimated by varying the b tagging scale factors within one standard deviation [53]. Effects of the uncertainty in the distribution of the number of pileup interactions are evaluated by varying the effective inelastic pp cross section used to predict the num-
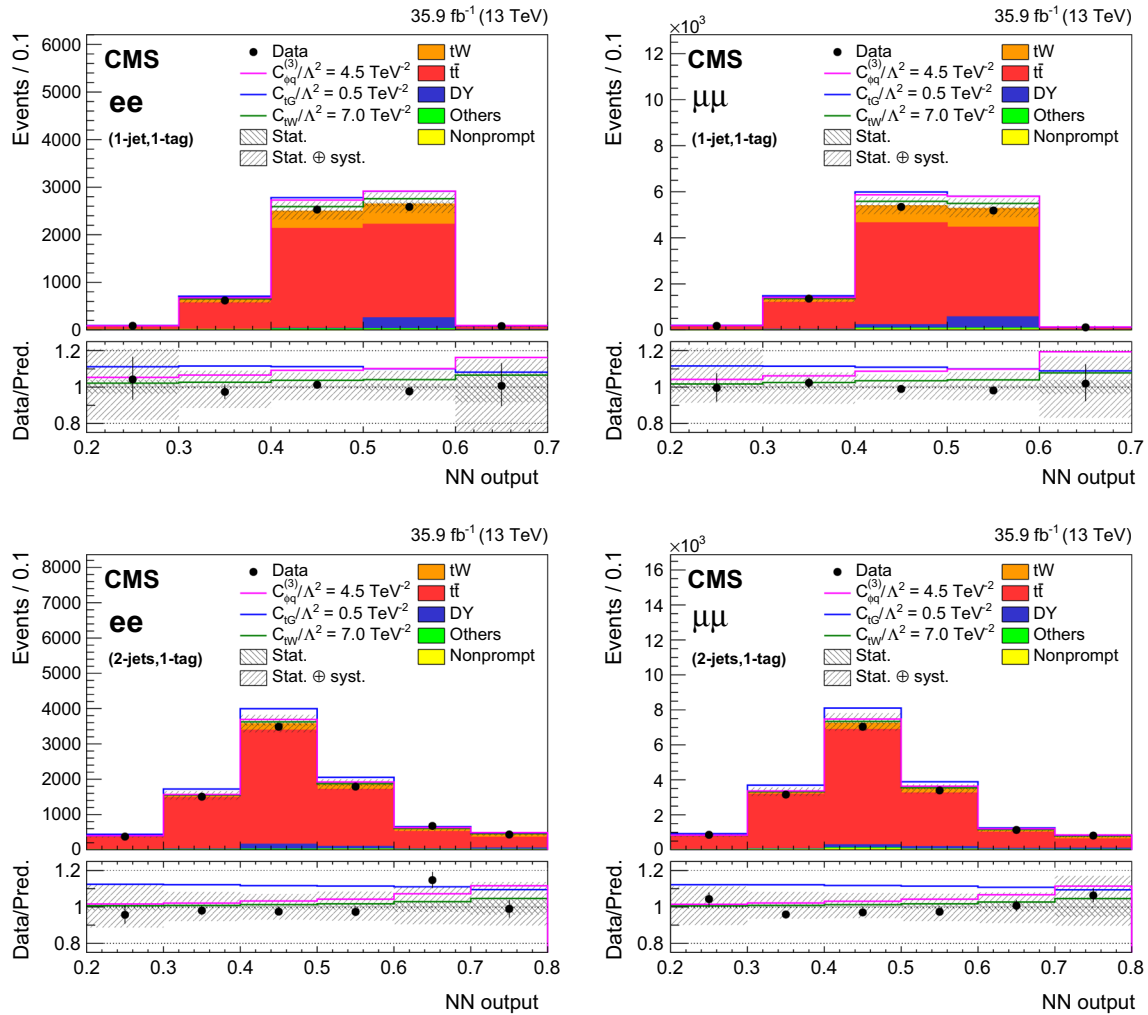
Fig. 3 The NN output distributions for data and simulation for the ee (left) and $\mu\mu$ (right) channels in 1-jet, 1-tag (upper) and 2-jets, 1-tag (lower) categories. The hatched bands correspond to the quadratic sum of the statistical and systematic uncertainties in the event yield for the sum of signal and background predictions. The ratios of data to the sum of the predicted yields are shown at the lower panel of each graph. The narrow hatched bands represent the contribution from the statistical uncertainty in the MC simulation. In each plot, the expected distributions assuming specific values for the effective couplings (given in the legend) are shown as the solid curves

ber of pileup interactions in MC simulation by $\pm 4.6\%$ of its nominal value [61].

The uncertainty in the DY contribution in categories with one or two b-tagged jets is considered to be 50 and 30% in the eμ and same-flavor dilepton channels, respectively [10,57]. For the DY normalization in the (1-jet, 0-tag) category, an uncertainty of 15% is assigned [62]. In addition, systematic uncertainties related to the PDF, and to the renormalization and factorization scale uncertainty are taken into account for DY process in the (1-jet, 0-tag) category. The uncertainty in the yield of nonprompt lepton backgrounds is considered to be 50% [57]. Contributions to the background from $t\bar{t}$ production in association with a boson, as well as diboson production, are estimated from simulation and a systematic uncertainty of 50% is conservatively assigned [63].

Various uncertainties originate from the theoretical predictions. The effect of the renormalization and factorization scale uncertainty from the $t\bar{t}$ and tW MC generators is estimated by varying the scales used during the generation of the simulation sample independently by a factor 0.5, 1 or 2. Unphysical cases, where one scale fluctuates up while the other fluctuates down, are not considered. The top quark p_T reweighting procedure, discussed in Sect. 2, is applied on top of the nominal POWHEG prediction at NLO to account for the higher-order corrections.

The uncertainty in the PDFs for each simulated signal process is obtained using the replicas of the NNPDF 3.0 set [64]. The most recent measurement of the top quark mass by CMS yields a total uncertainty of ± 0.49 GeV [65]. We consider variations of the top quark mass due to this uncertainty and
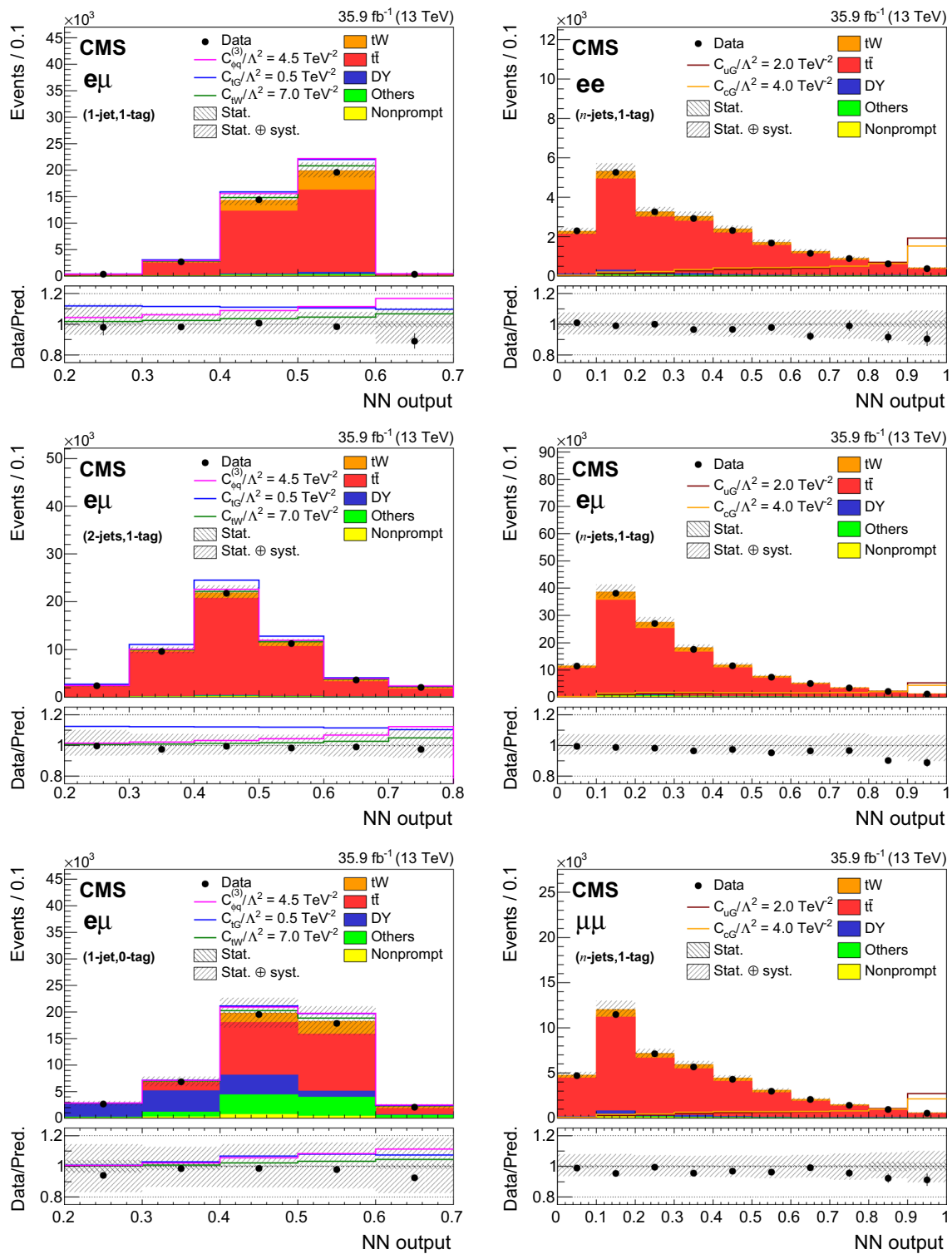
Fig. 4 The NN output distributions for (left) data and simulation for the eμ channel in 1-jet, 1-tag (upper) and 2-jets, 1-tag (middle) and 1-jet, 0-tag (lower) categories; and for (right) data, simulation, and FCNC signals in the *n*-jets, 1-tag category used in the limit setting for the ee (upper), eμ (middle), and μμ (lower) channels. The hatched bands correspond to the quadratic sum of the statistical and systematic uncer-tainties in the event yield for the sum of signal and background predic-tions. The ratios of data to the sum of the predicted yields are shown at the lower panel of each graph. The narrow hatched bands represent the contribution from the statistical uncertainty in the MC simulation. In each plot, the expected distributions assuming specific values for the effective couplings (given in the legend) are shown as the solid curves

Table 4 Input variables for the NN used in the analysis in various bins of n-jets and m-tags. The symbols "$\times$" indicate the input variables used in the four NNs

Variable	NN_{10}	NN_{11}	NN_{21}	NN_{FCNC}
$M_{\ell\ell}$	$\times$			$\times$
$p_T^{\ell\ell}$	$\times$		$\times$	$\times$
$\Delta p_T(\ell_1, \ell_2)$	$\times$			$\times$
$p_T^{\ell_1}$	$\times$		$\times$	$\times$
Centrality(ℓ_1, jet$_1$)	$\times$			$\times$
Centrality(ℓ_1, ℓ_2)	$\times$			$\times$
$\Delta\Phi(\ell\ell, \text{jet}_1)$	$\times$	$\times$	$\times$	
$p_T(\ell\ell, \text{jet}_1)$		$\times$		$\times$
$p_T(\ell_1, \text{jet}_1)$		$\times$		
Centrality($\ell\ell$, jet$_1$)		$\times$		
$\Delta R(\ell_1, \ell_2)$		$\times$		
$\Delta R(\ell_1, \text{jet}_1)$		$\times$		
$M(\ell_1, \text{jet}_1)$			$\times$	
$M(\text{jet}_1, \text{jet}_2)$			$\times$	
$\Delta R(\ell_1, \text{jet}_2)$			$\times$	
$\Delta R(\ell\ell, \text{jet}_1)$			$\times$	$\times$
$\Delta p_T(\ell_2, \text{jet}_2)$			$\times$	
$M(\ell_2, \text{jet}_1)$				$\times$

they are found to be insignificant. At NLO QCD, tW production is expected to interfere with t$\bar{\text{t}}$ production [66]. Two schemes for defining the tW signal in a way that distinguishes it from the t$\bar{\text{t}}$ production have been compared in the analysis: the "diagram removal" (DR), in which all doubly resonant NLO tW diagrams are removed, and the "diagram subtraction" (DS), where a gauge-invariant subtractive term modifies the NLO tW cross section to locally cancel the contribution from t$\bar{\text{t}}$ production [66–68]. The DR method is used for the nominal tW sample and the difference with respect to the sample simulated using the DS method is taken as a systematic uncertainty. The model parameter h_{damp} in t$\bar{\text{t}}$ POWHEG [25] that controls the matching of the matrix elements to the PYTHIA parton showers is varied from a top quark mass default value of 172.5 GeV by factors of 0.5 and 2 for estimating the uncertainties from the matching between jets from matrix element calculations and parton shower emissions. The renormalization scale for QCD emissions in the initial- and final-state radiation (ISR and FSR) is varied up and down by factors of 2 and $\sqrt{2}$, respectively, to account for parton shower QCD scale variation error in both t$\bar{\text{t}}$ and tW samples [69]. In addition, several dedicated t$\bar{\text{t}}$ samples are used to estimate shower modeling uncertainties in both underlying event and color re-connections [10,31,69]. To estimate model uncertainties, tW and t$\bar{\text{t}}$ samples are generated with POWHEG as described in Sect. 2, varying the relevant model parameters with respect to the nominal samples.

6 Constraints on the effective couplings

The six Wilson coefficients sensitive to new physics contributions in top quark interactions, as defined in Eqs. 1–5, are tested separately in the observed data. The event yields and the NN output distributions in each analysis category, summarized in Table 3, are used to construct a binned likelihood function. All sources of systematic uncertainty, described in Sect. 5, are taken into account as nuisance parameters in the fit. A simultaneous binned maximum-likelihood fit is performed to find the best fit value for each Wilson coefficient together with 68 and 95% confidence intervals (CIs) [70]. In this section, distributions of the log-likelihood functions are shown with one nonzero effective coupling at a time for $\Lambda = 1$ TeV.

The SM cross section prediction for the t$\bar{\text{t}}$ and tW processes, $\sigma_i^{(1)}$ and $\sigma_i^{(2)}$ (see Table 1), are accompanied by uncertainties in scales and PDFs. These theoretical uncertainties can affect the bounds on the Wilson coefficients. In order to study this effect, the fit is performed on data, while theoretical uncertainties are varied within one standard deviation and are shown together with the nominal results in the likelihood scan plots in Fig. 5. The nominal theoretical cross sections for t$\bar{\text{t}}$ and tW processes are varied by [+4.8%, −5.5%] and [+5.4%, −5.4%] , respectively. These variations cover the uncertainties arising from the variations of factorization and renormalization scales and PDFs [10,34]. The scale variations for $\sigma_i^{(1)}$ and $\sigma_i^{(2)}$ are evaluated to be within 1–25%. We assumed that the scale uncertainty is 100% correlated among the terms σ_{SM}, $\sigma_i^{(1)}$, and $\sigma_i^{(2)}$.

6.1 Exclusion limits on the C_G effective coupling

In order to constrain the C_G coupling, the effect on the t$\bar{\text{t}}$ rate in various (n-jets,m-tags) categories is considered. The impact of the difference between the kinematic distributions of t$\bar{\text{t}}$ events from the O_G interaction and from the SM interactions on the acceptance is evaluated to be 3% for $C_G \sim 1$. This uncertainty is considered only for the C_G coupling since the top p_T spectrum is affected considerably by this operator, while other operators lead to a p_T spectrum similar to the SM prediction for unconstrained values of the probed Wilson coefficients. The fit is performed simultaneously on the observed event yields in the categories presented in Fig. 2 in the (1-jet, 1-tag), (2-jets, 1-tag), and ($\geq$2-jets, 2-tags) categories for the ee, eμ, and $\mu\mu$ channels. In addition, the (1-jet, 0-tag) category is included only for the eμ channel. The main limiting factor on the constraints in the C_G coupling is the uncertainty in the signal acceptance found after maximizing the likelihood, followed by uncertainties in the integrated luminosity calibration and the trigger scale factor.

The results of the fit for the individual channels and for all channels combined are listed in the first row of Table 5.
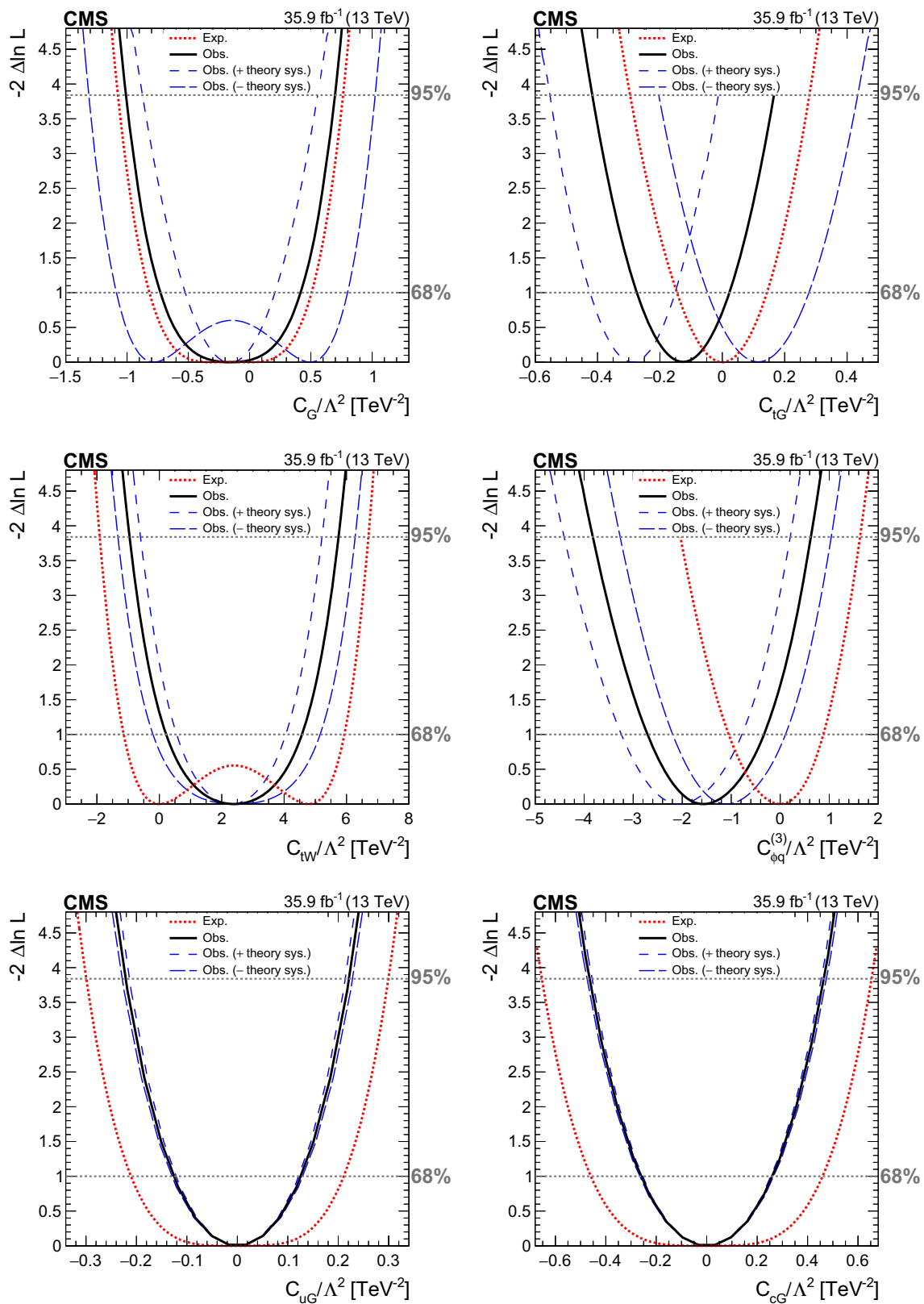
Fig. 5 Observed (solid) and expected (dotted) log likelihoods for the effective couplings: C_G (upper left), C_{tG} (upper right), C_{tW} (middle left), $C_{\phi q}$ (middle right), C_{uG} (lower left), and C_{cG} (lower right). The dashed curves represent fits to the observed data with the variations of normalization due to the theoretical uncertainties

Table 5 Summary of the observed and expected allowed intervals on the effective couplings obtained in the ee, eμ, and μμ channels, and all channels combined. All sources of systematic uncertainty, described in Sect. 5, are taken into account with the exception of the uncertainties on the SM cross section predictions for the tt and tW processes

Effective coupling	Channel	Observed [TeV^{-2}]			Expected [TeV^{-2}]		
		Best fit	[68% CI]	[95% CI]	Best fit	[68% CI]	[95% CI]
C_G/Λ^2	ee	−0.14	[−0.82, 0.51]	[−1.14, 0.83]	0.00	[−0.90, 0.59]	[−1.20, 0.88]
	eμ	−0.18	[−0.73, 0.42]	[−1.01, 0.70]	0.00	[−0.82, 0.51]	[−1.08, 0.77]
	μμ	−0.14	[−0.75, 0.44]	[−1.06, 0.75]	0.00	[−0.88, 0.57]	[−1.16, 0.85]
	Combined	−0.18	[−0.73, 0.42]	[−1.01, 0.70]	0.00	[−0.82, 0.51]	[−1.07, 0.76]
$C_{\phi q}^{(3)}/\Lambda^2$	ee	1.12	[−1.18, 2.89]	[−4.03, 4.37]	0.00	[−2.53, 1.74]	[−6.40, 3.27]
	eμ	−0.70	[−2.16, 0.59]	[−3.74, 1.61]	0.00	[−1.34, 1.12]	[−2.57, 2.15]
	μμ	1.13	[−0.87, 2.86]	[−3.58, 4.46]	0.00	[−2.20, 1.92]	[−4.68, 3.66]
	Combined	−1.52	[−2.71, −0.33]	[−3.82, 0.63]	0.00	[−1.05, 0.88]	[−2.04, 1.63]
C_{tW}/Λ^2	ee	6.18	[−3.02, 7.81]	[−4.16, 8.95]	0.00	[−2.02, 6.81]	[−3.33, 8.12]
	eμ	1.64	[−0.80, 5.59]	[−1.89, 6.68]	0.00	[−1.40, 6.19]	[−2.39, 7.18]
	μμ	−1.40	[−3.00, 7.79]	[−4.23, 9.01]	0.00	[−2.18, 6.97]	[−3.63, 8.42]
	Combined	2.38	[0.22, 4.57]	[−0.96, 5.74]	0.00	[−1.14, 5.93]	[−1.91, 6.70]
C_{tG}/Λ^2	ee	−0.19	[−0.40, 0.02]	[−0.65, 0.22]	0.00	[−0.22, 0.21]	[−0.44, 0.41]
	eμ	−0.03	[−0.19, 0.11]	[−0.34, 0.27]	0.00	[−0.17, 0.15]	[−0.34, 0.29]
	μμ	−0.15	[−0.34, 0.02]	[−0.53, 0.19]	0.00	[−0.19, 0.18]	[−0.40, 0.35]
	Combined	−0.13	[−0.27, 0.02]	[−0.41, 0.17]	0.00	[−0.15, 0.14]	[−0.30, 0.28]
C_{uG}/Λ^2	ee	−0.017	[−0.22, 0.22]	[−0.37, 0.37]	0.00	[−0.29, 0.29]	[−0.42, 0.42]
	eμ	−0.017	[−0.17, 0.17]	[−0.29, 0.29]	0.00	[−0.26, 0.26]	[−0.38, 0.38]
	μμ	−0.017	[−0.17, 0.17]	[−0.29, 0.29]	0.00	[−0.27, 0.27]	[−0.38, 0.38]
	Combined	−0.017	[−0.13, 0.13]	[−0.22, 0.22]	0.00	[−0.21, 0.21]	[−0.30, 0.30]
C_{cG}/Λ^2	ee	−0.032	[−0.47, 0.47]	[−0.78, 0.78]	0.00	[−0.63, 0.63]	[−0.92, 0.92]
	eμ	−0.032	[−0.34, 0.34]	[−0.60, 0.60]	0.00	[−0.56, 0.56]	[−0.81, 0.81]
	μμ	−0.032	[−0.36, 0.36]	[−0.63, 0.63]	0.00	[−0.58, 0.58]	[−0.84, 0.84]
	Combined	−0.032	[−0.26, 0.26]	[−0.46, 0.46]	0.00	[−0.46, 0.46]	[−0.65, 0.65]

The results of the likelihood scans of the C_G coupling are shown in Fig. 5 (upper left plot). The likelihood scan result of the nominal fit, in which the nominal values of σ_{SM}, $\sigma_i^{(1)}$, and $\sigma_i^{(2)}$ terms are assumed, is shown as the thick curve. The thin dashed curves are the results of the fit to the observed data when the assumed values of the σ_{SM}, $\sigma_i^{(1)}$, and $\sigma_i^{(2)}$ terms are varied due to the scale and PDF uncertainties. As a second-order parametrization, given by Eq. 6 is used to fit the data, the resulting likelihood function could have two minima, as can be seen in some of the plots in Fig. 5.

6.2 Exclusion limits on the C_{tG}, $C_{\phi q}^{(3)}$, and C_{tW} effective couplings

In order to set limits on the effective couplings C_{tG}, $C_{\phi q}^{(3)}$, and C_{tW}, we utilize the NN output distributions for both data and MC expectation in the (1-jet, 1-tag) and (2-jets, 1-tag) regions and event yields in the ($\geq$2-jets, 2-tags) region for the three dilepton channels. The inclusion of the ($\geq$2-jets,
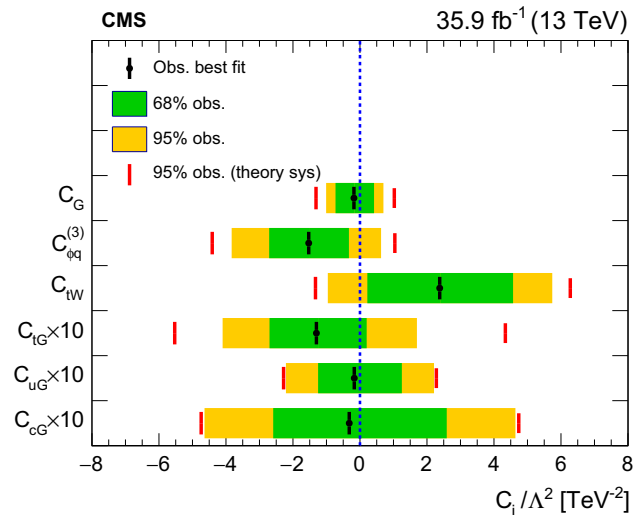

Fig. 6 Observed best fits together with one and two standard deviation bounds on the top quark effective couplings. The dashed line shows the SM expectation and the vertical lines indicate the 95% CL bounds including the theoretical uncertainties

Table 6 Estimation of the effect of the most important uncertainty sources on the observed allowed intervals of in the fit

Uncertainty	C_G (%)	$C_{\phi q}^{(3)}$ (%)	C_{tW} (%)	C_{tG} (%)	C_{uG} (%)	C_{cG} (%)
Trigger	10.2	2.3	7.0	2.9	1.7	2.5
Lepton ident./isolation	7.4	1.1	1.2	23.0	<1	<1
Jet energy scale	<1	25.0	17.8	4.9	<1	<1
tW DS/DR	<1	24.2	4.4	3.0	7.6	7.8
ME/PS matching	<1	4.9	9.9	1.2	<1	<1
ISR scale	<1	5.0	5.6	<1	<1	<1
FSR scale	5.8	4.4	4.0	10.2	<1	<1
DY background	<1	7.5	5.5	21.5	<1	<1
Nonprompt background	<1	1.4	5.8	<1	<1	<1
Integrated luminosity	13.1	<1	1.1	18.8	<1	<1
Statistical	5.8	2.3	23.7	<1	72.6	73.6
MC statistical	<1	12.1	3.7	5.2	2.9	2.5

2-tags) and (2-jets, 1-tag) categories provides a constraint of the normalization and systematic uncertainties in the $t\bar{t}$ background. In addition, the (1-jet, 0-tag) category is included for the eμ channel to increase the signal sensitivity. The results of the likelihood scans of the C_{tG}, $C_{\phi q}^{(3)}$, and C_{tW} Wilson coefficients are shown in Fig. 5 for the combination of all channels. The inclusion of the C_{tG} coupling to the tW process tightens the 2 standard deviations band by 7%. The results for the individual channels, and the combined results are listed in Table 5 (second, third, and fourth rows). The three main sources of uncertainty that affect the interval determination are uncertainties in the DY estimation, integrated luminosity, and lepton identification scale factors for C_{tG}; jet energy scale, tt and tW interference at NLO, and statistical uncertainty in MC samples for $C_{\phi q}^{(3)}$; statistical uncertainty in data, jet energy scale, and the POWHEG matching method for C_{tW} effective couplings.

6.3 Exclusion limits on the C_{uG} and C_{cG} effective couplings

Since the tW production via FCNC interactions does not interfere with the SM tW process (with the assumption of $|V_{td}| = |V_{ts}| = 0$), the FCNC signal sample is used to set upper bounds on the related Wilson coefficients. Events with exactly one b-tagged jet are included in the limit setting procedure with no requirement on the number of light-flavor jets (n-jets, 1-tag). The observed (median expected) 95% confidence level (CL) upper limits on the product of cross section times branching fractions $\sigma(pp \to tW)\mathcal{B}(W \to \ell\nu)^2$ for the C_{uG} and C_{cG} FCNC signals for the combination of the ee, μμ, and eμ channels are found to be 0.11 (0.20) pb and 0.13 (0.26) pb, respectively. These results are used to calculate upper limits on the Wilson coefficients C_{uG}, C_{cG}, and on the branching fractions $\mathcal{B}(t \to ug)$ and $\mathcal{B}(t \to cg)$. The limits on the C_{uG} and C_{cG} couplings are summarized in the last two

rows of Table 5, and correspond to the observed (expected) limits on $\mathcal{B}(t \to ug) < 0.12$ (0.22)% and $\mathcal{B}(t \to cg) < 0.53$ (1.05)% at 95% CL. The statistical uncertainty in data is the dominant source of uncertainty affecting the limits on the FCNC couplings. The second and third most important uncertainties originate from $t\bar{t}$ and tW interferences at NLO and FSR in $t\bar{t}$ events.

The observed best fit together with one and two standard deviation bounds on the six Wilson coefficients, $C_{\phi q}^{(3)}$, C_{tW}, C_{tG}, C_G, C_{uG}, and C_{cG}, obtained from the combination of all channels are shown in Fig. 6. Table 6 summarizes the effect of the most important uncertainty sources on the observed allowed intervals.

7 Summary

A search for new physics in top quark interactions is performed using $t\bar{t}$ and tW events in dilepton final states. The analysis is based on data collected in pp collisions at 13 TeV by the CMS detector in 2016, corresponding to an integrated luminosity of 35.9 fb^{-1}. No significant excess above the standard model background expectation is observed. For the first time, both $t\bar{t}$ and tW production are used simultaneously in a model independent search for effective couplings. The six effective couplings, C_G, C_{tG}, C_{tW}, $C_{\phi q}^{(3)}$, C_{uG}, and C_{cG} are constrained using a dedicated multivariate analysis. The constraints presented, obtained by considering one operator at a time, are a useful first step toward more global approaches.

Data Availability Statement This manuscript has no associated data or the data will not be deposited. [Authors' comment: Release and preservation of data used by the CMS Collaboration as the basis for publications is guided by the CMS policy as written in its document "CMS data preservation, reuse and open access policy" (https://cms-docdb.cern.ch/cgibin/PublicDocDB/RetrieveFile?docid=6032&filename=CMSDataPolicyV1.2.pdf&version=2).]

References

1. D0 Collaboration, Combination of searches for anomalous top quark couplings with 5.4 fb^{-1} of p$\bar{\text{p}}$ collisions. Phys. Lett. B **713**, 165 (2012). https://doi.org/10.1016/j.physletb.2012.05.048. arXiv:1204.2332

2. ATLAS Collaboration, Probing the Wtb vertex structure in t-channel single-top-quark production and decay in pp collisions at $\sqrt{s} = 8$ TeV with the ATLAS detector. JHEP **04**, 124 (2017). https://doi.org/10.1007/JHEP04(2017)124. arXiv:1702.08309

3. ATLAS Collaboration, Measurement of the W boson polarisation in t$\bar{\text{t}}$ events from pp collisions at $\sqrt{s} = 8$ TeV in the lepton+jets channel with ATLAS. Eur. Phys. J. C **77**, 264 (2017). https://doi.org/10.1140/epjc/s10052-017-4819-4. arXiv:1612.02577

4. CMS Collaboration, Search for anomalous Wtb couplings and flavour-changing neutral currents in t-channel single top quark production in pp collisions at $\sqrt{s} = 7$ and 8 TeV. JHEP **02**, 028 (2017). https://doi.org/10.1007/JHEP02(2017)028. arXiv:1610.03545

5. CMS Collaboration, Measurement of the W boson helicity in events with a single reconstructed top quark in pp collisions at $\sqrt{s} = 8$ TeV. JHEP **01**, 053 (2015). https://doi.org/10.1007/JHEP01(2015)053. arXiv:1410.1154

6. CMS Collaboration, Measurements of t$\bar{\text{t}}$ spin correlations and top quark polarization using dilepton final states in pp collisions at $\sqrt{s} = 8$ TeV. Phys. Rev. D **93**, 052007 (2016). https://doi.org/10.1103/PhysRevD.93.052007. arXiv:1601.01107

7. D0 Collaboration, Search for flavor changing neutral currents via quark-gluon couplings in single top quark production using 2.3 fb^{-1} of p$\bar{\text{p}}$ collisions. Phys. Lett. B **693**, 81 (2010). https://doi.org/10.1016/j.physletb.2010.08.011. arXiv:1006.3575

8. CDF Collaboration, Search for top-quark production via flavor-changing neutral currents in W+1 jet events at CDF. Phys. Rev. Lett. **102**, 151801 (2009). https://doi.org/10.1103/PhysRevLett.102.151801. arXiv:0812.3400

9. ATLAS Collaboration, Search for single top-quark production via flavour-changing neutral currents at 8 TeV with the ATLAS detector. Eur. Phys. J. C **76**, 55 (2016). https://doi.org/10.1140/epjc/s10052-016-3876-4. arXiv:1509.00294

10. CMS Collaboration, Measurements of t$\bar{\text{t}}$ differential cross sections in proton-proton collisions at $\sqrt{s} = 13$ TeV using events containing two leptons. JHEP **02**, 149 (2019). https://doi.org/10.1007/JHEP02(2019)149. arXiv:1811.06625

11. W. Buchmuller, D. Wyler, Effective Lagrangian analysis of new interactions and flavor conservation. Nucl. Phys. B **268**, 621 (1986). https://doi.org/10.1016/0550-3213(86)90262-2

12. B. Grzadkowski, M. Iskrzynski, M. Misiak, J. Rosiek, Dimension-six terms in the standard model Lagrangian. JHEP **10**, 085 (2010). https://doi.org/10.1007/JHEP10(2010)085. arXiv:1008.4884

13. C. Zhang, S. Willenbrock, Effective-field-theory approach to top-quark production and decay. Phys. Rev. D **83**, 034006 (2011). https://doi.org/10.1103/PhysRevD.83.034006. arXiv:1008.3869

14. A. Buckley et al., Constraining top quark effective theory in the LHC Run II era. JHEP **04**, 015 (2016). https://doi.org/10.1007/JHEP04(2016)015. arXiv:1512.03360

15. N.P. Hartland et al., A Monte Carlo global analysis of the standard model effective field theory: the top quark sector. JHEP **04**, 100 (2019). https://doi.org/10.1007/JHEP04(2019)100. arXiv:1901.05965

16. G. Durieux, F. Maltoni, C. Zhang, Global approach to top-quark flavor-changing interactions. Phys. Rev. D **91**, 074017 (2015). https://doi.org/10.1103/PhysRevD.91.074017. arXiv:1412.7166

17. J.A. Aguilar Saavedra et al., Interpreting top-quark LHC measurements in the standard-model effective field theory (2018). arXiv:1802.07237

18. R.M. Godbole, M.E. Peskin, S.D. Rindani, R.K. Singh, Why the angular distribution of the top decay lepton is unchanged by anomalous tbW couplings. Phys. Lett. B **790**, 322–325 (2019). https://doi.org/10.1016/j.physletb.2019.01.022. arXiv:1809.06285

19. A. Stange, S. Willenbrock, Yukawa correction to top quark production at the Tevatron. Phys. Rev. D **48**, 2054 (1993). https://doi.org/10.1103/PhysRevD.48.2054. arXiv:hep-ph/9302291

20. C.-S. Li, B.-Q. Hu, J.-M. Yang, C.-G. Hu, Supersymmetric QCD corrections to top quark production in p$\bar{\text{p}}$ collisions. Phys. Rev. D **52**, 5014 (1995). https://doi.org/10.1103/PhysRevD.52.5014. [Erratum: https://doi.org/10.1103/PhysRevD.53.4112]

21. F. Krauss, S. Kuttimalai, T. Plehn, LHC multijet events as a probe for anomalous dimension-six gluon interactions. Phys. Rev. D **95**, 035024 (2017). https://doi.org/10.1103/PhysRevD.95.035024. arXiv:1611.00767

22. P.L. Cho, E.H. Simmons, Searching for G^3 in $t\bar{t}$ production. Phys. Rev. D **51**, 2360 (1995). https://doi.org/10.1103/PhysRevD.51.2360. arXiv:hep-ph/9408206

23. V. Hirschi, F. Maltoni, I. Tsinikos, E. Vryonidou, Constraining anomalous gluon self-interactions at the LHC: a reappraisal. JHEP **07**, 093 (2018). https://doi.org/10.1007/JHEP07(2018)093. arXiv:1806.04696

24. CMS Collaboration, The CMS experiment at the CERN LHC. JINST **3**, S08004 (2008). https://doi.org/10.1088/1748-0221/3/08/S08004

25. S. Frixione, P. Nason, C. Oleari, Matching NLO QCD computations with parton shower simulations: the POWHEG method. JHEP **11**, 070 (2007). https://doi.org/10.1088/1126-6708/2007/11/070. arXiv:0709.2092

26. S. Alioli, P. Nason, C. Oleari, E. Re, A general framework for implementing NLO calculations in shower Monte Carlo programs: the POWHEG BOX. JHEP **06**, 043 (2010). https://doi.org/10.1007/JHEP06(2010)043. arXiv:1002.2581

27. E. Re, Single-top Wt-channel production matched with parton showers using the POWHEG method. Eur. Phys. J. C **71**, 1547 (2011). https://doi.org/10.1140/epjc/s10052-011-1547-z. arXiv:1009.2450

28. S. Alioli, P. Nason, C. Oleari, E. Re, NLO single-top production matched with shower in POWHEG: s- and t-channel contributions. JHEP **09**, 111 (2009). https://doi.org/10.1007/JHEP02(2010)011. arXiv:0907.4076

29. T. Sjöstrand et al., An introduction to PYTHIA 8.2. Comput. Phys. Commun. **191**, 159 (2015). https://doi.org/10.1016/j.cpc.2015.01.024. arXiv:1410.3012

30. CMS Collaboration, Event generator tunes obtained from underlying event and multiparton scattering measurements. Eur. Phys. J. C **76**, 155 (2016). https://doi.org/10.1140/epjc/s10052-016-3988-x. arXiv:1512.00815

31. CMS Collaboration, Investigations of the impact of the parton shower tuning in PYTHIA 8 in the modelling of $t\bar{t}$ at $\sqrt{s} = 8$ and 13 TeV. CMS Physics Analysis Summary CMS-PAS-TOP-16-021 (2016)

32. NNPDF Collaboration, Parton distributions for the LHC Run II. JHEP **04**, 040 (2015). https://doi.org/10.1007/JHEP04(2015)040. arXiv:1410.8849

33. M. Czakon, A. Mitov, Top++: a program for the calculation of the top-pair cross-section at hadron colliders. Comput. Phys. Commun. **185**, 2930 (2014). https://doi.org/10.1016/j.cpc.2014.06.021. arXiv:1112.5675

34. N. Kidonakis, Theoretical results for electroweak-boson and single-top production, in *Proceedings, 23rd International Workshop on Deep-Inelastic Scattering and Related Subjects (DIS 2015)*. Dallas, April, 2015, PoS(DIS2015)170, p. 170. https://doi.org/10.22323/1.247.0170. arXiv:1506.04072.

35. M. Czakon et al., Top-pair production at the LHC through NNLO QCD and NLO EW. JHEP **10**, 186 (2017). https://doi.org/10.1007/JHEP10(2017)186. arXiv:1705.04105

36. J. Alwall et al., MadGraph/MadEvent v4: the new web generation. JHEP **09**, 028 (2007). https://doi.org/10.1088/1126-6708/2007/09/028. arXiv:0706.2334

37. J. Alwall et al., The automated computation of tree-level and next-to-leading order differential cross sections, and their matching to parton shower simulations. JHEP **07**, 079 (2014). https://doi.org/10.1007/JHEP07(2014)079. arXiv:1405.0301

38. R. Frederix, S. Frixione, Merging meets matching in MC@NLO. JHEP **12**, 061 (2012). https://doi.org/10.1007/JHEP12(2012)061. arXiv:1209.6215

39. GEANT4 Collaboration, GEANT4—a simulation toolkit. Nucl. Instrum. Methods A **506**, 250 (2003). https://doi.org/10.1016/S0168-9002(03)01368-8

40. J. Allison et al., GEANT4 developments and applications. IEEE Trans. Nucl. Sci. **53**, 270 (2006). https://doi.org/10.1109/TNS.2006.869826

41. C. Degrande et al., UFO—the universal feynRules output. Comput. Phys. Commun. **183**, 1201 (2012). https://doi.org/10.1016/j.cpc.2012.01.022. arXiv:1108.2040

42. A. Alloul et al., FeynRules 2.0—a complete toolbox for tree-level phenomenology. Comput. Phys. Commun. **185**, 2250 (2014). https://doi.org/10.1016/j.cpc.2014.04.012. arXiv:1310.1921

43. D.B. Franzosi, C. Zhang, Probing the top-quark chromomagnetic dipole moment at next-to-leading order in QCD. Phys. Rev. D **91**, 114010 (2015). https://doi.org/10.1103/PhysRevD.91.114010. arXiv:1503.08841

44. C. Zhang, Single top production at next-to-leading order in the standard model effective field theory. Phys. Rev. Lett. **116**, 162002 (2016). https://doi.org/10.1103/PhysRevLett.116.162002. arXiv:1601.06163

45. CMS Collaboration, The CMS trigger system. JINST **12**, P01020 (2017). https://doi.org/10.1088/1748-0221/12/01/P01020. arXiv:1609.02366

46. CMS Collaboration, Particle-flow reconstruction and global event description with the CMS detector. JINST **12**, P10003 (2017). https://doi.org/10.1088/1748-0221/12/10/P10003. arXiv:1706.04965

47. CMS Collaboration, Performance of electron reconstruction and selection with the CMS detector in proton-proton collisions at $\sqrt{s} = 8$ TeV. JINST **10**, P06005 (2015). https://doi.org/10.1088/1748-0221/10/06/P06005. arXiv:1502.02701

48. CMS Collaboration, Performance of the CMS muon detector and muon reconstruction with proton-proton collisions at $\sqrt{s} = 13$ TeV. JINST **13**, P06015 (2018). https://doi.org/10.1088/1748-0221/13/06/P06015. arXiv:1804.04528

49. M. Cacciari, G.P. Salam, G. Soyez, FastJet user manual. Eur. Phys. J. C **72**, 1896 (2012). https://doi.org/10.1140/epjc/s10052-012-1896-2. arXiv:1111.6097

50. M. Cacciari, G.P. Salam, G. Soyez, The anti-k_t jet clustering algorithm. JHEP **04**, 063 (2008). https://doi.org/10.1088/1126-6708/2008/04/063. arXiv:0802.1189

51. M. Cacciari, G.P. Salam, Dispelling the N^3 myth for the k_t jet-finder. Phys. Lett. B **641**, 57 (2006). https://doi.org/10.1016/j.physletb.2006.08.037. arXiv:hep-ph/0512210

52. CMS Collaboration, Jet energy scale and resolution in the CMS experiment in pp collisions at 8 TeV. JINST **12**, P02014 (2017). https://doi.org/10.1088/1748-0221/12/02/P02014. arXiv:1607.03663

53. CMS Collaboration, Identification of heavy-flavour jets with the CMS detector in pp collisions at 13 TeV. JINST **13**, P05011 (2018). https://doi.org/10.1088/1748-0221/13/05/P05011. arXiv:1712.07158

54. CMS Collaboration, Performance of the CMS missing transverse momentum reconstruction in pp data at $\sqrt{s} = 8$ TeV. JINST **10**, P02006 (2015). https://doi.org/10.1088/1748-0221/10/02/P02006. arXiv:1411.0511

55. CMS Collaboration, First measurement of the cross section for top-quark pair production in proton-proton collisions at $\sqrt{s} = 7$ TeV. Phys. Lett. B **695**, 424 (2011). https://doi.org/10.1016/j.physletb.2010.11.058. arXiv:1010.5994

56. B.H. Denby, The use of neural networks in high-energy physics. Neural Comput. **5**, 505 (1993). https://doi.org/10.1162/neco.1993.5.4.505

57. CMS Collaboration, Measurement of the production cross section for single top quarks in association with W bosons in proton-proton collisions at $\sqrt{s} = 13$ TeV. JHEP **10**, 117 (2018). https://doi.org/10.1007/JHEP10(2018)117. arXiv:1805.07399

60. CMS Collaboration, Determination of jet energy calibration and transverse momentum resolution in CMS. JINST **6**, P11002 (2011). https://doi.org/10.1088/1748-0221/6/11/P11002. arXiv:1107.4277

61. CMS Collaboration, Measurement of the inelastic proton-proton cross section at $\sqrt{s} = 13$ TeV. JHEP **07**, 161 (2018). https://doi.org/10.1007/JHEP07(2018)161. arXiv:1802.02613

62. CMS Collaboration, Measurement of differential cross sections for Z boson production in association with jets in proton-proton collisions at $\sqrt{s} = 13$ TeV. Eur. Phys. J. C **78**, 965 (2018). https://doi.org/10.1140/epjc/s10052-018-6373-0. arXiv:1804.05252

63. CMS Collaboration, Measurement of the cross section for top quark pair production in association with a W or Z boson in proton-proton collisions at $\sqrt{s} = 13$ TeV. JHEP **08**, 011 (2018). https://doi.org/10.1007/JHEP08(2018)011. arXiv:1711.02547

64. J. Butterworth et al., PDF4LHC recommendations for LHC Run II. J. Phys. G **43**, 023001 (2016). https://doi.org/10.1088/0954-3899/43/2/023001. arXiv:1510.03865

65. CMS Collaboration, Measurement of the top quark mass using proton-proton data at $\sqrt{s} = 7$ and 8 TeV. Phys. Rev. D **93**, 072004 (2016). https://doi.org/10.1103/PhysRevD.93.072004. arXiv:1509.04044

66. S. Frixione et al., Single-top hadroproduction in association with a W boson. JHEP **07**, 029 (2008). https://doi.org/10.1088/1126-6708/2008/07/029. arXiv:0805.3067

67. J.M. Campbell, F. Tramontano, Next-to-leading order corrections to Wt production and decay. Nucl. Phys. B **726**, 109 (2005). https://doi.org/10.1016/j.nuclphysb.2005.08.015. arXiv:hep-ph/0506289

68. A. Belyaev, E. Boos, Single top quark tW+X production at the CERN LHC: a closer look. Phys. Rev. D **63**, 034012 (2001). https://doi.org/10.1103/PhysRevD.63.034012. arXiv:hep-ph/0003260

69. P. Skands, S. Carrazza, J. Rojo, Tuning PYTHIA 8.1: the Monash 2013 tune. Eur. Phys. J. C **74**, 3024 (2014). https://doi.org/10.1140/epjc/s10052-014-3024-y. arXiv:1404.5630

70. CMS Collaboration, Precise determination of the mass of the Higgs boson and tests of compatibility of its couplings with the standard model predictions using proton collisions at 7 and 8 TeV. Eur. Phys. J. C **75**, 212 (2015). https://doi.org/10.1140/epjc/s10052-015-3351-7. arXiv:1412.8662

CMS Collaboration

Yerevan Physics Institute, Yerevan, Armenia
A. M. Sirunyan, A. Tumasyan

Institut für Hochenergiephysik, Vienna, Austria
W. Adam, F. Ambrogi, E. Asilar, T. Bergauer, J. Brandstetter, M. Dragicevic, J. Erö, A. Escalante Del Valle, M. Flechl, R. Frühwirth[1], V. M. Ghete, J. Hrubec, M. Jeitler[1], N. Krammer, I. Krätschmer, D. Liko, T. Madlener, I. Mikulec, N. Rad, H. Rohringer, J. Schieck[1], R. Schöfbeck, M. Spanring, D. Spitzbart, W. Waltenberger, J. Wittmann, C.-E. Wulz[1], M. Zarucki

Institute for Nuclear Problems, Minsk, Belarus
V. Chekhovsky, V. Mossolov, J. Suarez Gonzalez

Universiteit Antwerpen, Antwerp, Belgium
E. A. De Wolf, D. Di Croce, X. Janssen, J. Lauwers, A. Lelek, M. Pieters, H. Van Haevermaet, P. Van Mechelen, N. Van Remortel

Vrije Universiteit Brussel, Brussels, Belgium
S. Abu Zeid, F. Blekman, J. D'Hondt, J. De Clercq, K. Deroover, G. Flouris, D. Lontkovskyi, S. Lowette, I. Marchesini, S. Moortgat, L. Moreels, Q. Python, K. Skovpen, S. Tavernier, W. Van Doninck, P. Van Mulders, I. Van Parijs

Université Libre de Bruxelles, Brussels, Belgium
D. Beghin, B. Bilin, H. Brun, B. Clerbaux, G. De Lentdecker, H. Delannoy, B. Dorney, G. Fasanella, L. Favart, A. Grebenyuk, A. K. Kalsi, T. Lenzi, J. Luetic, N. Postiau, E. Starling, L. Thomas, C. Vander Velde, P. Vanlaer, D. Vannerom, Q. Wang

Ghent University, Ghent, Belgium
T. Cornelis, D. Dobur, A. Fagot, M. Gul, I. Khvastunov[2], D. Poyraz, C. Roskas, D. Trocino, M. Tytgat, W. Verbeke, B. Vermassen, M. Vit, N. Zaganidis

Université Catholique de Louvain, Louvain-la-Neuve, Belgium
H. Bakhshiansohi, O. Bondu, G. Bruno, C. Caputo, P. David, C. Delaere, M. Delcourt, A. Giammanco, G. Krintiras, V. Lemaitre, A. Magitteri, K. Piotrzkowski, A. Saggio, M. Vidal Marono, P. Vischia, J. Zobec

Centro Brasileiro de Pesquisas Fisicas, Rio de Janeiro, Brazil
F. L. Alves, G. A. Alves, G. Correia Silva, C. Hensel, A. Moraes, M. E. Pol, P. Rebello Teles

Universidade do Estado do Rio de Janeiro, Rio de Janeiro, Brazil

E. Belchior Batista Das Chagas, W. Carvalho, J. Chinellato[3], E. Coelho, E. M. Da Costa, G. G. Da Silveira[4], D. De Jesus Damiao, C. De Oliveira Martins, S. Fonseca De Souza, H. Malbouisson, D. Matos Figueiredo, M. Melo De Almeida, C. Mora Herrera, L. Mundim, H. Nogima, W. L. Prado Da Silva, L. J. Sanchez Rosas, A. Santoro, A. Sznajder, M. Thiel, E. J. Tonelli Manganote[3], F. Torres Da Silva De Araujo, A. Vilela Pereira

Universidade Estadual Paulista[a], Universidade Federal do ABC[b], São Paulo, Brazil

S. Ahuja[a], C. A. Bernardes[a], L. Calligaris[a], T. R. Fernandez Perez Tomei[a], E. M. Gregores[b], P. G. Mercadante[b], S. F. Novaes[a], Sandra S. Padula[a]

Institute for Nuclear Research and Nuclear Energy, Bulgarian Academy of Sciences, Sofia, Bulgaria

A. Aleksandrov, R. Hadjiiska, P. Iaydjiev, A. Marinov, M. Misheva, M. Rodozov, M. Shopova, G. Sultanov

University of Sofia, Sofia, Bulgaria

A. Dimitrov, L. Litov, B. Pavlov, P. Petkov

Beihang University, Beijing, China

W. Fang[5], X. Gao[5], L. Yuan

Institute of High Energy Physics, Beijing, China

M. Ahmad, J. G. Bian, G. M. Chen, H. S. Chen, M. Chen, Y. Chen, C. H. Jiang, D. Leggat, H. Liao, Z. Liu, S. M. Shaheen[6], A. Spiezia, J. Tao, E. Yazgan, H. Zhang, S. Zhang[6], J. Zhao

State Key Laboratory of Nuclear Physics and Technology, Peking University, Beijing, China

Y. Ban, G. Chen, A. Levin, J. Li, L. Li, Q. Li, Y. Mao, S. J. Qian, D. Wang

Tsinghua University, Beijing, China

Y. Wang

Universidad de Los Andes, Bogotá, Colombia

C. Avila, A. Cabrera, C. A. Carrillo Montoya, L. F. Chaparro Sierra, C. Florez, C. F. González Hernández, M. A. Segura Delgado

Faculty of Electrical Engineering, Mechanical Engineering and Naval Architecture, University of Split, Split, Croatia

B. Courbon, N. Godinovic, D. Lelas, I. Puljak, T. Sculac

Faculty of Science, University of Split, Split, Croatia

Z. Antunovic, M. Kovac

Institute Rudjer Boskovic, Zagreb, Croatia

V. Brigljevic, D. Ferencek, K. Kadija, B. Mesic, M. Roguljic, A. Starodumov[7], T. Susa

University of Cyprus, Nicosia, Cyprus

M. W. Ather, A. Attikis, M. Kolosova, G. Mavromanolakis, J. Mousa, C. Nicolaou, F. Ptochos, P. A. Razis, H. Rykaczewski

Charles University, Prague, Czech Republic

M. Finger[8], M. Finger Jr.[8]

Escuela Politecnica Nacional, Quito, Ecuador

E. Ayala

Universidad San Francisco de Quito, Quito, Ecuador

E. Carrera Jarrin

Academy of Scientific Research and Technology of the Arab Republic of Egypt, Egyptian Network of High Energy Physics, Cairo, Egypt

H. Abdalla[9], A. Mohamedj[10], E. Salama[11,12]

National Institute of Chemical Physics and Biophysics, Tallinn, Estonia

S. Bhowmik, A. Carvalho Antunes De Oliveira, R. K. Dewanjee, K. Ehataht, M. Kadastik, M. Raidal, C. Veelken

Department of Physics, University of Helsinki, Helsinki, Finland
P. Eerola, H. Kirschenmann, J. Pekkanen, M. Voutilainen

Helsinki Institute of Physics, Helsinki, Finland
J. Havukainen, J. K. Heikkilä, T. Järvinen, V. Karimäki, R. Kinnunen, T. Lampén, K. Lassila-Perini, S. Laurila, S. Lehti,
T. Lindén, P. Luukka, T. Mäenpää, H. Siikonen, E. Tuominen, J. Tuominiemi

Lappeenranta University of Technology, Lappeenranta, Finland
T. Tuuva

IRFU, CEA, Université Paris-Saclay, Gif-sur-Yvette, France
M. Besancon, F. Couderc, M. Dejardin, D. Denegri, J. L. Faure, F. Ferri, S. Ganjour, A. Givernaud, P. Gras,
G. Hamel de Monchenault, P. Jarry, C. Leloup, E. Locci, J. Malcles, G. Negro, J. Rander, A. Rosowsky, M. Ö. Sahin,
M. Titov

Laboratoire Leprince-Ringuet, Ecole polytechnique, CNRS/IN2P3, Université Paris-Saclay, Palaiseau, France
A. Abdulsalam[13], C. Amendola, I. Antropov, F. Beaudette, P. Busson, C. Charlot, R. Granier de Cassagnac, I. Kucher,
A. Lobanov, J. Martin Blanco, C. Martin Perez, M. Nguyen, C. Ochando, G. Ortona, P. Paganini, J. Rembser, R. Salerno,
J. B. Sauvan, Y. Sirois, A. G. Stahl Leiton, A. Zabi, A. Zghiche

Université de Strasbourg, CNRS, IPHC UMR 7178, Strasbourg, France
J.-L. Agram[14], J. Andrea, D. Bloch, G. Bourgatte, J.-M. Brom, E. C. Chabert, V. Cherepanov, C. Collard, E. Conte[14],
J.-C. Fontaine[14], D. Gelé, U. Goerlach, M. Jansová, A.-C. Le Bihan, N. Tonon, P. Van Hove

Centre de Calcul de l'Institut National de Physique Nucleaire et de Physique des Particules, CNRS/IN2P3, Villeurbanne, France
S. Gadrat

Université de Lyon, Université Claude Bernard Lyon 1, CNRS-IN2P3, Institut de Physique Nucléaire de Lyon, Villeurbanne, France
S. Beauceron, C. Bernet, G. Boudoul, N. Chanon, R. Chierici, D. Contardo, P. Depasse, H. El Mamouni, J. Fay, L. Finco,
S. Gascon, M. Gouzevitch, G. Grenier, B. Ille, F. Lagarde, I. B. Laktineh, H. Lattaud, M. Lethuillier, L. Mirabito,
S. Perries, A. Popov[15], V. Sordini, G. Touquet, M. Vander Donckt, S. Viret

Georgian Technical University, Tbilisi, Georgia
T. Toriashvili[16]

Tbilisi State University, Tbilisi, Georgia
Z. Tsamalaidze[8]

I. Physikalisches Institut, RWTH Aachen University, Aachen, Germany
C. Autermann, L. Feld, M. K. Kiesel, K. Klein, M. Lipinski, M. Preuten, M. P. Rauch, C. Schomakers, J. Schulz,
M. Teroerde, B. Wittmer

III. Physikalisches Institut A, RWTH Aachen University, Aachen, Germany
A. Albert, M. Erdmann, S. Erdweg, T. Esch, R. Fischer, S. Ghosh, T. Hebbeker, C. Heidemann, K. Hoepfner, H. Keller,
L. Mastrolorenzo, M. Merschmeyer, A. Meyer, P. Millet, S. Mukherjee, T. Pook, A. Pozdnyakov, M. Radziej, H. Reithler,
M. Rieger, A. Schmidt, D. Teyssier, S. Thüer

III. Physikalisches Institut B, RWTH Aachen University, Aachen, Germany
G. Flügge, O. Hlushchenko, T. Kress, T. Müller, A. Nehrkorn, A. Nowack, C. Pistone, O. Pooth, D. Roy, H. Sert, A. Stahl[17]

Deutsches Elektronen-Synchrotron, Hamburg, Germany
M. Aldaya Martin, T. Arndt, C. Asawatangtrakuldee, I. Babounikau, K. Beernaert, O. Behnke, U. Behrens,
A. Bermúdez Martínez, D. Bertsche, A. A. Bin Anuar, K. Borras[18], V. Botta, A. Campbell, P. Connor,
C. Contreras-Campana, V. Danilov, A. De Wit, M. M. Defranchis, C. Diez Pardos, D. Domínguez Damiani, G. Eckerlin,
T. Eichhorn, A. Elwood, E. Eren, E. Gallo[19], A. Geiser, J. M. Grados Luyando, A. Grohsjean, M. Guthoff, M. Haranko,
A. Harb, H. Jung, M. Kasemann, J. Keaveney, C. Kleinwort, J. Knolle, D. Krücker, W. Lange, T. Lenz, J. Leonard,
K. Lipka, W. Lohmann[20], R. Mankel, I.-A. Melzer-Pellmann, A. B. Meyer, M. Meyer, M. Missiroli, G. Mittag, J. Mnich,

V. Myronenko, S. K. Pflitsch, D. Pitzl, A. Raspereza, A. Saibel, M. Savitskyi, P. Saxena, P. Schütze, C. Schwanenberger, R. Shevchenko, A. Singh, H. Tholen, O. Turkot, A. Vagnerini, M. Van De Klundert, G. P. Van Onsem, R. Walsh, Y. Wen, K. Wichmann, C. Wissing, O. Zenaiev

University of Hamburg, Hamburg, Germany
R. Aggleton, S. Bein, L. Benato, A. Benecke, T. Dreyer, A. Ebrahimi, E. Garutti, D. Gonzalez, P. Gunnellini, J. Haller, A. Hinzmann, A. Karavdina, G. Kasieczka, R. Klanner, R. Kogler, N. Kovalchuk, S. Kurz, V. Kutzner, J. Lange, D. Marconi, J. Multhaup, M. Niedziela, C. E. N. Niemeyer, D. Nowatschin, A. Perieanu, A. Reimers, O. Rieger, C. Scharf, P. Schleper, S. Schumann, J. Schwandt, J. Sonneveld, H. Stadie, G. Steinbrück, F. M. Stober, M. Stöver, B. Vormwald, I. Zoi

Karlsruher Institut fuer Technologie, Karlsruhe, Germany
M. Akbiyik, C. Barth, M. Baselga, S. Baur, E. Butz, R. Caspart, T. Chwalek, F. Colombo, W. De Boer, A. Dierlamm, K. El Morabit, N. Faltermann, B. Freund, M. Giffels, M. A. Harrendorf, F. Hartmann[17], S. M. Heindl, U. Husemann, I. Katkov[15], S. Kudella, S. Mitra, M. U. Mozer, Th. Müller, M. Musich, M. Plagge, G. Quast, K. Rabbertz, M. Schröder, I. Shvetsov, H. J. Simonis, R. Ulrich, S. Wayand, M. Weber, T. Weiler, C. Wöhrmann, R. Wolf

Institute of Nuclear and Particle Physics (INPP), NCSR Demokritos, Aghia Paraskevi, Greece
G. Anagnostou, G. Daskalakis, T. Geralis, A. Kyriakis, D. Loukas, G. Paspalaki

National and Kapodistrian University of Athens, Athens, Greece
A. Agapitos, G. Karathanasis, P. Kontaxakis, A. Panagiotou, I. Papavergou, N. Saoulidou, K. Vellidis

National Technical University of Athens, Athens, Greece
K. Kousouris, I. Papakrivopoulos, G. Tsipolitis

University of Ioánnina, Ioánnina, Greece
I. Evangelou, C. Foudas, P. Gianneios, P. Katsoulis, P. Kokkas, S. Mallios, N. Manthos, I. Papadopoulos, E. Paradas, J. Strologas, F. A. Triantis, D. Tsitsonis

MTA-ELTE Lendület CMS Particle and Nuclear Physics Group, Eötvös Loránd University, Budapest, Hungary
M. Bartók[21], M. Csanad, N. Filipovic, P. Major, M. I. Nagy, G. Pasztor, O. Surányi, G. I. Veres

Wigner Research Centre for Physics, Budapest, Hungary
G. Bencze, C. Hajdu, D. Horvath[22], Á. Hunyadi, F. Sikler, T. Á. Vámi, V. Veszpremi, G. Vesztergombi[†]

Institute of Nuclear Research ATOMKI, Debrecen, Hungary
N. Beni, S. Czellar, J. Karancsi[21], A. Makovec, J. Molnar, Z. Szillasi

Institute of Physics, University of Debrecen, Debrecen, Hungary
P. Raics, Z. L. Trocsanyi, B. Ujvari

Indian Institute of Science (IISc), Bangalore, India
S. Choudhury, J. R. Komaragiri, P. C. Tiwari

National Institute of Science Education and Research, HBNI, Bhubaneswar, India
S. Bahinipati[24], C. Kar, P. Mal, K. Mandal, A. Nayak[25], S. Roy Chowdhury, D. K. Sahoo[24], S. K. Swain

Panjab University, Chandigarh, India
S. Bansal, S. B. Beri, V. Bhatnagar, S. Chauhan, R. Chawla, N. Dhingra, R. Gupta, A. Kaur, M. Kaur, S. Kaur, P. Kumari, M. Lohan, M. Meena, A. Mehta, K. Sandeep, S. Sharma, J. B. Singh, A. K. Virdi, G. Walia

University of Delhi, Delhi, India
A. Bhardwaj, B. C. Choudhary, R. B. Garg, M. Gola, S. Keshri, A. Kumar, S. Malhotra, M. Naimuddin, P. Priyanka, K. Ranjan, A. Shah, R. Sharma

Saha Institute of Nuclear Physics, HBNI, Kolkata, India
R. Bhardwaj[26], M. Bharti[26], R. Bhattacharya, S. Bhattacharya, U. Bhawandeep[26], D. Bhowmik, S. Dey, S. Dutt[26], S. Dutta, S. Ghosh, M. Maity[27], K. Mondal, S. Nandan, A. Purohit, P. K. Rout, A. Roy, G. Saha, S. Sarkar, T. Sarkar[27], M. Sharan, B. Singh[26], S. Thakur[26]

Indian Institute of Technology Madras, Madras, India
P. K. Behera, A. Muhammad

Bhabha Atomic Research Centre, Mumbai, India
R. Chudasama, D. Dutta, V. Jha, V. Kumar, D. K. Mishra, P. K. Netrakanti, L. M. Pant, P. Shukla, P. Suggisetti

Tata Institute of Fundamental Research-A, Mumbai, India
T. Aziz, M. A. Bhat, S. Dugad, G. B. Mohanty, N. Sur, R. Verma

Tata Institute of Fundamental Research-B, Mumbai, India
S. Banerjee, S. Bhattacharya, S. Chatterjee, P. Das, M. Guchait, Sa. Jain, S. Karmakar, S. Kumar, G. Majumder,
K. Mazumdar, N. Sahoo

Indian Institute of Science Education and Research (IISER), Pune, India
S. Chauhan, S. Dube, V. Hegde, A. Kapoor, K. Kothekar, S. Pandey, A. Rane, A. Rastogi, S. Sharma

Institute for Research in Fundamental Sciences (IPM), Tehran, Iran
S. Chenarani[28], E. Eskandari Tadavani, S. M. Etesami[28], M. Khakzad, M. Mohammadi Najafabadi, M. Naseri,
F. Rezaei Hosseinabadi, B. Safarzadeh[29], M. Zeinali

University College Dublin, Dublin, Ireland
M. Felcini, M. Grunewald

INFN Sezione di Bari[a], Università di Bari[b], Politecnico di Bari[c], Bari, Italy
M. Abbrescia[a,b], C. Calabria[a,b], A. Colaleo[a], D. Creanza[a,c], L. Cristella[a,b], N. De Filippis[a,c], M. De Palma[a,b],
A. Di Florio[a,b], F. Errico[a,b], L. Fiore[a], A. Gelmi[a,b], G. Iaselli[a,c], M. Ince[a,b], S. Lezki[a,b], G. Maggi[a,c], M. Maggi[a],
G. Miniello[a,b], S. My[a,b], S. Nuzzo[a,b], A. Pompili[a,b], G. Pugliese[a,c], R. Radogna[a], A. Ranieri[a], G. Selvaggi[a,b],
A. Sharma[a], L. Silvestris[a], R. Venditti[a], P. Verwilligen[a]

INFN Sezione di Bologna[a], Università di Bologna[b], Bologna, Italy
G. Abbiendi[a], C. Battilana[a,b], D. Bonacorsi[a,b], L. Borgonovi[a,b], S. Braibant-Giacomelli[a,b], R. Campanini[a,b],
P. Capiluppi[a,b], A. Castro[a,b], F. R. Cavallo[a], S. S. Chhibra[a,b], G. Codispoti[a,b], M. Cuffiani[a,b], G. M. Dallavalle[a],
F. Fabbri[a], A. Fanfani[a,b], E. Fontanesi, P. Giacomelli[a], C. Grandi[a], L. Guiducci[a,b], F. Iemmi[a,b], S. Lo Meo[a,30],
S. Marcellini[a], G. Masetti[a], A. Montanari[a], F. L. Navarria[a,b], A. Perrotta[a], F. Primavera[a,b], A. M. Rossi[a,b], T. Rovelli[a,b],
G. P. Siroli[a,b], N. Tosi[a]

INFN Sezione di Catania[a], Università di Catania[b], Catania, Italy
S. Albergo[a,b], A. Di Mattia[a], R. Potenza[a,b], A. Tricomi[a,b], C. Tuve[a,b]

INFN Sezione di Firenze[a], Università di Firenze[b], Florence, Italy
G. Barbagli[a], K. Chatterjee[a,b], V. Ciulli[a,b], C. Civinini[a], R. D'Alessandro[a,b], E. Focardi[a,b], G. Latino, P. Lenzi[a,b],
M. Meschini[a], S. Paoletti[a], L. Russo[a,31], G. Sguazzoni[a], D. Strom[a], L. Viliani[a]

INFN Laboratori Nazionali di Frascati, Frascati, Italy
L. Benussi, S. Bianco, F. Fabbri, D. Piccolo

INFN Sezione di Genova[a], Università di Genova[b], Genoa, Italy
F. Ferro[a], R. Mulargia[a,b], E. Robutti[a], S. Tosi[a,b]

INFN Sezione di Milano-Bicocca[a], Università di Milano-Bicocca[b], Milan, Italy
A. Benaglia[a], A. Beschi[b], F. Brivio[a,b], V. Ciriolo[a,b,17], S. Di Guida[a,b,17], M. E. Dinardo[a,b], S. Fiorendi[a,b], S. Gennai[a],
A. Ghezzi[a,b], P. Govoni[a,b], M. Malberti[a,b], S. Malvezzi[a], D. Menasce[a], F. Monti, L. Moroni[a], M. Paganoni[a,b],
D. Pedrini[a], S. Ragazzi[a,b], T. Tabarelli de Fatis[a,b], D. Zuolo[a,b]

**INFN Sezione di Napoli[a], Università di Napoli 'Federico II'[b], Naples, Italy, Università della Basilicata[c], Potenza,
Italy, Università G. Marconi[d], Rome, Italy**
S. Buontempo[a], N. Cavallo[a,c], A. De Iorio[a,b], A. Di Crescenzo[a,b], F. Fabozzi[a,c], F. Fienga[a], G. Galati[a], A. O. M. Iorio[a,b],
L. Lista[a], S. Meola[a,d,17], P. Paolucci[a,17], C. Sciacca[a,b], E. Voevodina[a,b]

INFN Sezione di Padova[a], Università di Padova[b], Padova, Italy, Università di Trento[c], Trento, Italy

P. Azzi[a], N. Bacchetta[a], D. Bisello[a,b], A. Boletti[a,b], A. Bragagnolo, R. Carlin[a,b], P. Checchia[a], M. Dall'Osso[a,b], P. De Castro Manzano[a], T. Dorigo[a], U. Dosselli[a], F. Gasparini[a,b], U. Gasparini[a,b], A. Gozzelino[a], S. Y. Hoh, S. Lacaprara[a], P. Lujan, M. Margoni[a,b], A. T. Meneguzzo[a,b], J. Pazzini[a,b], M. Presilla[b], P. Ronchese[a,b], R. Rossin[a,b], F. Simonetto[a,b], A. Tiko, E. Torassa[a], M. Tosi[a,b], M. Zanetti[a,b], P. Zotto[a,b], G. Zumerle[a,b]

INFN Sezione di Pavia[a], Università di Pavia[b], Pavia, Italy

A. Braghieri[a], A. Magnani[a], P. Montagna[a,b], S. P. Ratti[a,b], V. Re[a], M. Ressegotti[a,b], C. Riccardi[a,b], P. Salvini[a], I. Vai[a,b], P. Vitulo[a,b]

INFN Sezione di Perugia[a], Università di Perugia[b], Perugia, Italy

M. Biasini[a,b], G. M. Bilei[a], C. Cecchi[a,b], D. Ciangottini[a,b], L. Fanò[a,b], P. Lariccia[a,b], R. Leonardi[a,b], E. Manoni[a], G. Mantovani[a,b], V. Mariani[a,b], M. Menichelli[a], A. Rossi[a,b], A. Santocchia[a,b], D. Spiga[a]

INFN Sezione di Pisa[a], Università di Pisa[b], Scuola Normale Superiore di Pisa[c], Pisa, Italy

K. Androsov[a], P. Azzurri[a], G. Bagliesi[a], L. Bianchini[a], T. Boccali[a], L. Borrello, R. Castaldi[a], M. A. Ciocci[a,b], R. Dell'Orso[a], G. Fedi[a], F. Fiori[a,c], L. Giannini[a,c], A. Giassi[a], M. T. Grippo[a], F. Ligabue[a,c], E. Manca[a,c], G. Mandorli[a,c], A. Messineo[a,b], F. Palla[a], A. Rizzi[a,b], G. Rolandi[32], P. Spagnolo[a], R. Tenchini[a], G. Tonelli[a,b], A. Venturi[a], P. G. Verdini[a]

INFN Sezione di Roma[a], Sapienza Università di Roma[b], Rome, Italy

L. Barone[a,b], F. Cavallari[a], M. Cipriani[a,b], D. Del Re[a,b], E. Di Marco[a,b], M. Diemoz[a], S. Gelli[a,b], E. Longo[a,b], B. Marzocchi[a,b], P. Meridiani[a], G. Organtini[a,b], F. Pandolfi[a], R. Paramatti[a,b], F. Preiato[a,b], S. Rahatlou[a,b], C. Rovelli[a], F. Santanastasio[a,b]

INFN Sezione di Torino[a], Università di Torino[b], Torino, Italy, Università del Piemonte Orientale[c], Novara, Italy

N. Amapane[a,b], R. Arcidiacono[a,c], S. Argiro[a,b], M. Arneodo[a,c], N. Bartosik[a], R. Bellan[a,b], C. Biino[a], A. Cappati[a,b], N. Cartiglia[a], F. Cenna[a,b], S. Cometti, M. Costa[a,b], R. Covarelli[a,b], N. Demaria[a], B. Kiani[a,b], C. Mariotti[a], S. Maselli[a], E. Migliore[a,b], V. Monaco[a,b], E. Monteil[a,b], M. Monteno[a], M. M. Obertino[a,b], L. Pacher[a,b], N. Pastrone[a], M. Pelliccioni[a], G. L. Pinna Angioni[a,b], A. Romero[a,b], M. Ruspa[a,c], R. Sacchi[a,b], R. Salvatico[a,b], K. Shchelina[a,b], V. Sola[a], A. Solano[a,b], D. Soldi[a,b], A. Staiano[a]

INFN Sezione di Trieste[a], Università di Trieste[b], Trieste, Italy

S. Belforte[a], V. Candelise[a,b], M. Casarsa[a], F. Cossutti[a], A. Da Rold[a,b], G. Della Ricca[a,b], F. Vazzoler[a,b], A. Zanetti[a]

Kyungpook National University, Daegu, Korea

D. H. Kim, G. N. Kim, M. S. Kim, J. Lee, S. Lee, S. W. Lee, C. S. Moon, Y. D. Oh, S. I. Pak, S. Sekmen, D. C. Son, Y. C. Yang

Institute for Universe and Elementary Particles, Chonnam National University, Kwangju, Korea

H. Kim, D. H. Moon, G. Oh

Hanyang University, Seoul, Korea

B. Francois, J. Goh[33], T. J. Kim

Korea University, Seoul, Korea

S. Cho, S. Choi, Y. Go, D. Gyun, S. Ha, B. Hong, Y. Jo, K. Lee, K. S. Lee, S. Lee, J. Lim, S. K. Park, Y. Roh

Sejong University, Seoul, Korea

H. S. Kim

Seoul National University, Seoul, Korea

J. Almond, J. Kim, J. S. Kim, H. Lee, K. Lee, K. Nam, S. B. Oh, B. C. Radburn-Smith, S. h. Seo, U. K. Yang, H. D. Yoo, G. B. Yu

University of Seoul, Seoul, Korea

D. Jeon, H. Kim, J. H. Kim, J. S. H. Lee, I. C. Park

Sungkyunkwan University, Suwon, Korea

Y. Choi, C. Hwang, J. Lee, I. Yu

Riga Technical University, Riga, Latvia
V. Veckalns[34]

Vilnius University, Vilnius, Lithuania
V. Dudenas, A. Juodagalvis, J. Vaitkus

National Centre for Particle Physics, Universiti Malaya, Kuala Lumpur, Malaysia
Z. A. Ibrahim, M. A. B. Md Ali[35], F. Mohamad Idris[36], W. A. T. Wan Abdullah, M. N. Yusli, Z. Zolkapli

Universidad de Sonora (UNISON), Hermosillo, Mexico
J. F. Benitez, A. Castaneda Hernandez, J. A. Murillo Quijada

Centro de Investigacion y de Estudios Avanzados del IPN, Mexico City, Mexico
H. Castilla-Valdez, E. De La Cruz-Burelo, M. C. Duran-Osuna, I. Heredia-De La Cruz[37], R. Lopez-Fernandez,
J. Mejia Guisao, R. I. Rabadan-Trejo, M. Ramirez-Garcia, G. Ramirez-Sanchez, R. Reyes-Almanza, A. Sanchez-Hernandez

Universidad Iberoamericana, Mexico City, Mexico
S. Carrillo Moreno, C. Oropeza Barrera, F. Vazquez Valencia

Benemerita Universidad Autonoma de Puebla, Puebla, Mexico
J. Eysermans, I. Pedraza, H. A. Salazar Ibarguen, C. Uribe Estrada

Universidad Autónoma de San Luis Potosí, San Luis Potosí, Mexico
A. Morelos Pineda

University of Auckland, Auckland, New Zealand
D. Krofcheck

University of Canterbury, Christchurch, New Zealand
S. Bheesette, P. H. Butler

National Centre for Physics, Quaid-I-Azam University, Islamabad, Pakistan
A. Ahmad, M. Ahmad, M. I. Asghar, Q. Hassan, H. R. Hoorani, W. A. Khan, M. A. Shah, M. Shoaib, M. Waqas

National Centre for Nuclear Research, Swierk, Poland
H. Bialkowska, M. Bluj, B. Boimska, T. Frueboes, M. Górski, M. Kazana, M. Szleper, P. Traczyk, P. Zalewski

Institute of Experimental Physics, Faculty of Physics, University of Warsaw, Warsaw, Poland
K. Bunkowski, A. Byszuk[38], K. Doroba, A. Kalinowski, M. Konecki, J. Krolikowski, M. Misiura, M. Olszewski,
A. Pyskir, M. Walczak

Laboratório de Instrumentação e Física Experimental de Partículas, Lisbon, Portugal
M. Araujo, P. Bargassa, C. Beirão Da Cruz E Silva, A. Di Francesco, P. Faccioli, B. Galinhas, M. Gallinaro, J. Hollar,
N. Leonardo, J. Seixas, G. Strong, O. Toldaiev, J. Varela

Joint Institute for Nuclear Research, Dubna, Russia
S. Afanasiev, P. Bunin, M. Gavrilenko, I. Golutvin, I. Gorbunov, A. Kamenev, V. Karjavine, A. Lanev, A. Malakhov,
V. Matveev[39,40], P. Moisenz, V. Palichik, V. Perelygin, S. Shmatov, S. Shulha, N. Skatchkov, V. Smirnov, N. Voytishin,
A. Zarubin

Petersburg Nuclear Physics Institute, Gatchina (St. Petersburg), Russia
V. Golovtsov, Y. Ivanov, V. Kim[41], E. Kuznetsova[42], P. Levchenko, V. Murzin, V. Oreshkin, I. Smirnov, D. Sosnov,
V. Sulimov, L. Uvarov, S. Vavilov, A. Vorobyev

Institute for Nuclear Research, Moscow, Russia
Yu. Andreev, A. Dermenev, S. Gninenko, N. Golubev, A. Karneyeu, M. Kirsanov, N. Krasnikov, A. Pashenkov,
A. Shabanov, D. Tlisov, A. Toropin

Institute for Theoretical and Experimental Physics, Moscow, Russia
V. Epshteyn, V. Gavrilov, N. Lychkovskaya, V. Popov, I. Pozdnyakov, G. Safronov, A. Spiridonov, A. Stepennov,
V. Stolin, M. Toms, E. Vlasov, A. Zhokin

Moscow Institute of Physics and Technology, Moscow, Russia
T. Aushev

National Research Nuclear University 'Moscow Engineering Physics Institute' (MEPhI), Moscow, Russia
R. Chistov[43], M. Danilov[43], D. Philippov, E. Tarkovskii

P.N. Lebedev Physical Institute, Moscow, Russia
V. Andreev, M. Azarkin, I. Dremin[40], M. Kirakosyan, A. Terkulov

Skobeltsyn Institute of Nuclear Physics, Lomonosov Moscow State University, Moscow, Russia
A. Baskakov, A. Belyaev, E. Boos, V. Bunichev, M. Dubinin[44], L. Dudko, V. Klyukhin, O. Kodolova, N. Korneeva,
I. Lokhtin, S. Obraztsov, M. Perfilov, V. Savrin

Novosibirsk State University (NSU), Novosibirsk, Russia
A. Barnyakov[45], V. Blinov[45], T. Dimova[45], L. Kardapoltsev[45], Y. Skovpen[45]

Institute for High Energy Physics of National Research Centre 'Kurchatov Institute', Protvino, Russia
I. Azhgirey, I. Bayshev, S. Bitioukov, V. Kachanov, A. Kalinin, D. Konstantinov, P. Mandrik, V. Petrov, R. Ryutin,
S. Slabospitskii, A. Sobol, S. Troshin, N. Tyurin, A. Uzunian, A. Volkov

National Research Tomsk Polytechnic University, Tomsk, Russia
A. Babaev, S. Baidali, V. Okhotnikov

Faculty of Physics and VINCA Institute of Nuclear Sciences, University of Belgrade, Belgrade, Serbia
P. Adzic[46], P. Cirkovic, D. Devetak, M. Dordevic, P. Milenovic[47], J. Milosevic

Centro de Investigaciones Energéticas Medioambientales y Tecnológicas (CIEMAT), Madrid, Spain
J. Alcaraz Maestre, A. Álvarez Fernández, I. Bachiller, M. Barrio Luna, J. A. Brochero Cifuentes, M. Cerrada, N. Colino,
B. De La Cruz, A. Delgado Peris, C. Fernandez Bedoya, J. P. Fernández Ramos, J. Flix, M. C. Fouz, O. Gonzalez Lopez,
S. Goy Lopez, J. M. Hernandez, M. I. Josa, D. Moran, A. Pérez-Calero Yzquierdo, J. Puerta Pelayo, I. Redondo,
L. Romero, S. Sánchez Navas, M. S. Soares, A. Triossi

Universidad Autónoma de Madrid, Madrid, Spain
C. Albajar, J. F. de Trocóniz

Universidad de Oviedo, Oviedo, Spain
J. Cuevas, C. Erice, J. Fernandez Menendez, S. Folgueras, I. Gonzalez Caballero, J. R. González Fernández,
E. Palencia Cortezon, V. Rodríguez Bouza, S. Sanchez Cruz, J. M. Vizan Garcia

Instituto de Física de Cantabria (IFCA), CSIC-Universidad de Cantabria, Santander, Spain
I. J. Cabrillo, A. Calderon, B. Chazin Quero, J. Duarte Campderros, M. Fernandez, P. J. Fernández Manteca,
A. García Alonso, J. Garcia-Ferrero, G. Gomez, A. Lopez Virto, J. Marco, C. Martinez Rivero, P. Martinez Ruiz del Arbol,
F. Matorras, J. Piedra Gomez, C. Prieels, T. Rodrigo, A. Ruiz-Jimeno, L. Scodellaro, N. Trevisani, I. Vila,
R. Vilar Cortabitarte

Department of Physics, University of Ruhuna, Matara, Sri Lanka
N. Wickramage

CERN, European Organization for Nuclear Research, Geneva, Switzerland
D. Abbaneo, B. Akgun, E. Auffray, G. Auzinger, P. Baillon, A. H. Ball, D. Barney, J. Bendavid, M. Bianco, A. Bocci,
C. Botta, E. Brondolin, T. Camporesi, M. Cepeda, G. Cerminara, E. Chapon, Y. Chen, G. Cucciati, D. d'Enterria,
A. Dabrowski, N. Daci, V. Daponte, A. David, A. De Roeck, N. Deelen, M. Dobson, M. Dünser, N. Dupont,
A. Elliott-Peisert, F. Fallavollita[48], D. Fasanella, G. Franzoni, J. Fulcher, W. Funk, D. Gigi, A. Gilbert, K. Gill, F. Glege,
M. Gruchala, M. Guilbaud, D. Gulhan, J. Hegeman, C. Heidegger, V. Innocente, G. M. Innocenti, A. Jafari, P. Janot,
O. Karacheban[20], J. Kieseler, A. Kornmayer, M. Krammer[1], C. Lange, P. Lecoq, C. Lourenço, L. Malgeri, M. Mannelli,
A. Massironi, F. Meijers, J. A. Merlin, S. Mersi, E. Meschi, F. Moortgat, M. Mulders, J. Ngadiuba, S. Nourbakhsh,
S. Orfanelli, L. Orsini, F. Pantaleo[17], L. Pape, E. Perez, M. Peruzzi, A. Petrilli, G. Petrucciani, A. Pfeiffer, M. Pierini,
F. M. Pitters, D. Rabady, A. Racz, M. Rovere, H. Sakulin, C. Schäfer, C. Schwick, M. Selvaggi, A. Sharma, P. Silva,
P. Sphicas[49], A. Stakia, J. Steggemann, D. Treille, A. Tsirou, A. Vartak, M. Verzetti, W. D. Zeuner

Paul Scherrer Institut, Villigen, Switzerland
L. Caminada[50], K. Deiters, W. Erdmann, R. Horisberger, Q. Ingram, H. C. Kaestli, D. Kotlinski, U. Langenegger, T. Rohe, S. A. Wiederkehr

ETH Zurich-Institute for Particle Physics and Astrophysics (IPA), Zurich, Switzerland
M. Backhaus, L. Bäni, P. Berger, N. Chernyavskaya, G. Dissertori, M. Dittmar, M. Donegà, C. Dorfer, T. A. Gómez Espinosa, C. Grab, D. Hits, T. Klijnsma, W. Lustermann, R. A. Manzoni, M. Marionneau, M. T. Meinhard, F. Micheli, P. Musella, F. Nessi-Tedaldi, F. Pauss, G. Perrin, L. Perrozzi, S. Pigazzini, M. Reichmann, C. Reissel, D. Ruini, D. A. Sanz Becerra, M. Schönenberger, L. Shchutska, V. R. Tavolaro, K. Theofilatos, M. L. Vesterbacka Olsson, R. Wallny, D. H. Zhu

Universität Zürich, Zurich, Switzerland
T. K. Aarrestad, C. Amsler[51], D. Brzhechko, M. F. Canelli, A. De Cosa, R. Del Burgo, S. Donato, C. Galloni, T. Hreus, B. Kilminster, S. Leontsinis, I. Neutelings, G. Rauco, P. Robmann, D. Salerno, K. Schweiger, C. Seitz, Y. Takahashi, S. Wertz, A. Zucchetta

National Central University, Chung-Li, Taiwan
T. H. Doan, R. Khurana, C. M. Kuo, W. Lin, S. S. Yu

National Taiwan University (NTU), Taipei, Taiwan
P. Chang, Y. Chao, K. F. Chen, P. H. Chen, W.-S. Hou, Y. F. Liu, R.-S. Lu, E. Paganis, A. Psallidas, A. Steen

Department of Physics, Faculty of Science, Chulalongkorn University, Bangkok, Thailand
B. Asavapibhop, N. Srimanobhas, N. Suwonjandee

Physics Department, Science and Art Faculty, Çukurova University, Adana, Turkey
A. Bat, F. Boran, S. Cerci[52], S. Damarseckin, Z. S. Demiroglu, F. Dolek, C. Dozen, I. Dumanoglu, E. Eskut, G. Gokbulut, Y. Guler, E. Gurpinar, I. Hos[53], C. Isik, E. E. Kangal[54], O. Kara, A. Kayis Topaksu, U. Kiminsu, M. Oglakci, G. Onengut, K. Ozdemir[55], A. Polatoz, D. Sunar Cerci[52], U. G. Tok, S. Turkcapar, I. S. Zorbakir, C. Zorbilmez

Physics Department, Middle East Technical University, Ankara, Turkey
B. Isildak[56], G. Karapinar[57], M. Yalvac, M. Zeyrek

Bogazici University, Istanbul, Turkey
I. O. Atakisi, E. Gülmez, M. Kaya[58], O. Kaya[59], S. Ozkorucuklu[60], S. Tekten, E. A. Yetkin[61]

Istanbul Technical University, Istanbul, Turkey
M. N. Agaras, A. Cakir, K. Cankocak, Y. Komurcu, S. Sen[62]

Institute for Scintillation Materials of National Academy of Science of Ukraine, Kharkov, Ukraine
B. Grynyov

National Scientific Center, Kharkov Institute of Physics and Technology, Kharkov, Ukraine
L. Levchuk

University of Bristol, Bristol, United Kingdom
F. Ball, J. J. Brooke, D. Burns, E. Clement, D. Cussans, O. Davignon, H. Flacher, J. Goldstein, G. P. Heath, H. F. Heath, L. Kreczko, D. M. Newbold[63], S. Paramesvaran, B. Penning, T. Sakuma, D. Smith, V. J. Smith, J. Taylor, A. Titterton

Rutherford Appleton Laboratory, Didcot, United Kingdom
K. W. Bell, A. Belyaev[64], C. Brew, R. M. Brown, D. Cieri, D. J. A. Cockerill, J. A. Coughlan, K. Harder, S. Harper, J. Linacre, K. Manolopoulos, E. Olaiya, D. Petyt, T. Reis, T. Schuh, C. H. Shepherd-Themistocleous, A. Thea, I. R. Tomalin, T. Williams, W. J. Womersley

Imperial College, London, United Kingdom
R. Bainbridge, P. Bloch, J. Borg, S. Breeze, O. Buchmuller, A. Bundock, D. Colling, P. Dauncey, G. Davies, M. Della Negra, R. Di Maria, P. Everaerts, G. Hall, G. Iles, T. James, M. Komm, C. Laner, L. Lyons, A.-M. Magnan, S. Malik, A. Martelli, J. Nash[65], A. Nikitenko[7], V. Palladino, M. Pesaresi, D. M. Raymond, A. Richards, A. Rose, E. Scott, C. Seez, A. Shtipliyski, G. Singh, M. Stoye, T. Strebler, S. Summers, A. Tapper, K. Uchida, T. Virdee[17], N. Wardle, D. Winterbottom, J. Wright, S. C. Zenz

Brunel University, Uxbridge, United Kingdom
J. E. Cole, P. R. Hobson, A. Khan, P. Kyberd, C. K. Mackay, A. Morton, I. D. Reid, L. Teodorescu, S. Zahid

Baylor University, Waco, USA
K. Call, J. Dittmann, K. Hatakeyama, H. Liu, C. Madrid, B. McMaster, N. Pastika, C. Smith

Catholic University of America, Washington DC, USA
R. Bartek, A. Dominguez

The University of Alabama, Tuscaloosa, USA
A. Buccilli, S. I. Cooper, C. Henderson, P. Rumerio, C. West

Boston University, Boston, USA
D. Arcaro, T. Bose, Z. Demiragli, D. Gastler, S. Girgis, D. Pinna, C. Richardson, J. Rohlf, D. Sperka, I. Suarez, L. Sulak, D. Zou

Brown University, Providence, USA
G. Benelli, B. Burkle, X. Coubez, D. Cutts, M. Hadley, J. Hakala, U. Heintz, J. M. Hogan[66], K. H. M. Kwok, E. Laird, G. Landsberg, J. Lee, Z. Mao, M. Narain, S. Sagir[67], R. Syarif, E. Usai, D. Yu

University of California, Davis, Davis, USA
R. Band, C. Brainerd, R. Breedon, D. Burns, M. Calderon De La Barca Sanchez, M. Chertok, J. Conway, R. Conway, P. T. Cox, R. Erbacher, C. Flores, G. Funk, W. Ko, O. Kukral, R. Lander, M. Mulhearn, D. Pellett, J. Pilot, S. Shalhout, M. Shi, D. Stolp, D. Taylor, K. Tos, M. Tripathi, Z. Wang, F. Zhang

University of California, Los Angeles, USA
M. Bachtis, C. Bravo, R. Cousins, A. Dasgupta, S. Erhan, A. Florent, J. Hauser, M. Ignatenko, N. Mccoll, S. Regnard, D. Saltzberg, C. Schnaible, V. Valuev

University of California, Riverside, Riverside, USA
E. Bouvier, K. Burt, R. Clare, J. W. Gary, S. M. A. Ghiasi Shirazi, G. Hanson, G. Karapostoli, E. Kennedy, F. Lacroix, O. R. Long, M. Olmedo Negrete, M. I. Paneva, W. Si, L. Wang, H. Wei, S. Wimpenny, B. R. Yates

University of California, San Diego, La Jolla, USA
J. G. Branson, P. Chang, S. Cittolin, M. Derdzinski, R. Gerosa, D. Gilbert, B. Hashemi, A. Holzner, D. Klein, G. Kole, V. Krutelyov, J. Letts, M. Masciovecchio, S. May, D. Olivito, S. Padhi, M. Pieri, V. Sharma, M. Tadel, J. Wood, F. Würthwein, A. Yagil, G. Zevi Della Porta

Department of Physics, University of California, Santa Barbara, Santa Barbara, USA
N. Amin, R. Bhandari, C. Campagnari, M. Citron, V. Dutta, M. Franco Sevilla, L. Gouskos, R. Heller, J. Incandela, H. Mei, A. Ovcharova, H. Qu, J. Richman, D. Stuart, S. Wang, J. Yoo

California Institute of Technology, Pasadena, USA
D. Anderson, A. Bornheim, J. M. Lawhorn, N. Lu, H. B. Newman, T. Q. Nguyen, J. Pata, M. Spiropulu, J. R. Vlimant, R. Wilkinson, S. Xie, Z. Zhang, R. Y. Zhu

Carnegie Mellon University, Pittsburgh, USA
M. B. Andrews, T. Ferguson, T. Mudholkar, M. Paulini, M. Sun, I. Vorobiev, M. Weinberg

University of Colorado Boulder, Boulder, USA
J. P. Cumalat, W. T. Ford, F. Jensen, A. Johnson, E. MacDonald, T. Mulholland, R. Patel, A. Perloff, K. Stenson, K. A. Ulmer, S. R. Wagner

Cornell University, Ithaca, USA
J. Alexander, J. Chaves, Y. Cheng, J. Chu, A. Datta, K. Mcdermott, N. Mirman, J. R. Patterson, D. Quach, A. Rinkevicius, A. Ryd, L. Skinnari, L. Soffi, S. M. Tan, Z. Tao, J. Thom, J. Tucker, P. Wittich, M. Zientek

Fermi National Accelerator Laboratory, Batavia, USA

S. Abdullin, M. Albrow, M. Alyari, G. Apollinari, A. Apresyan, A. Apyan, S. Banerjee, L. A. T. Bauerdick, A. Beretvas, J. Berryhill, P. C. Bhat, K. Burkett, J. N. Butler, A. Canepa, G. B. Cerati, H. W. K. Cheung, F. Chlebana, M. Cremonesi, J. Duarte, V. D. Elvira, J. Freeman, Z. Gecse, E. Gottschalk, L. Gray, D. Green, S. Grünendahl, O. Gutsche, J. Hanlon, R. M. Harris, S. Hasegawa, J. Hirschauer, Z. Hu, B. Jayatilaka, S. Jindariani, M. Johnson, U. Joshi, B. Klima, M. J. Kortelainen, B. Kreis, S. Lammel, D. Lincoln, R. Lipton, M. Liu, T. Liu, J. Lykken, K. Maeshima, J. M. Marraffino, D. Mason, P. McBride, P. Merkel, S. Mrenna, S. Nahn, V. O'Dell, K. Pedro, C. Pena, O. Prokofyev, G. Rakness, F. Ravera, A. Reinsvold, L. Ristori, A. Savoy-Navarro[68], B. Schneider, E. Sexton-Kennedy, A. Soha, W. J. Spalding, L. Spiegel, S. Stoynev, J. Strait, N. Strobbe, L. Taylor, S. Tkaczyk, N. V. Tran, L. Uplegger, E. W. Vaandering, C. Vernieri, M. Verzocchi, R. Vidal, M. Wang, H. A. Weber

University of Florida, Gainesville, USA

D. Acosta, P. Avery, P. Bortignon, D. Bourilkov, A. Brinkerhoff, L. Cadamuro, A. Carnes, D. Curry, R. D. Field, S. V. Gleyzer, B. M. Joshi, J. Konigsberg, A. Korytov, K. H. Lo, P. Ma, K. Matchev, N. Menendez, G. Mitselmakher, D. Rosenzweig, K. Shi, J. Wang, S. Wang, X. Zuo

Florida International University, Miami, USA

Y. R. Joshi, S. Linn

Florida State University, Tallahassee, USA

A. Ackert, T. Adams, A. Askew, S. Hagopian, V. Hagopian, K. F. Johnson, T. Kolberg, G. Martinez, T. Perry, H. Prosper, A. Saha, C. Schiber, R. Yohay

Florida Institute of Technology, Melbourne, USA

M. M. Baarmand, V. Bhopatkar, S. Colafranceschi, M. Hohlmann, D. Noonan, M. Rahmani, T. Roy, M. Saunders, F. Yumiceva

University of Illinois at Chicago (UIC), Chicago, USA

M. R. Adams, L. Apanasevich, D. Berry, R. R. Betts, R. Cavanaugh, X. Chen, S. Dittmer, O. Evdokimov, C. E. Gerber, D. A. Hangal, D. J. Hofman, K. Jung, J. Kamin, C. Mills, M. B. Tonjes, N. Varelas, H. Wang, X. Wang, Z. Wu, J. Zhang

The University of Iowa, Iowa City, USA

M. Alhusseini, B. Bilki[69], W. Clarida, K. Dilsiz[70], S. Durgut, R. P. Gandrajula, M. Haytmyradov, V. Khristenko, J.-P. Merlo, A. Mestvirishvili, A. Moeller, J. Nachtman, H. Ogul[71], Y. Onel, F. Ozok[72], A. Penzo, C. Snyder, E. Tiras, J. Wetzel

Johns Hopkins University, Baltimore, USA

B. Blumenfeld, A. Cocoros, N. Eminizer, D. Fehling, L. Feng, A. V. Gritsan, W. T. Hung, P. Maksimovic, J. Roskes, U. Sarica, M. Swartz, M. Xiao

The University of Kansas, Lawrence, USA

A. Al-bataineh, P. Baringer, A. Bean, S. Boren, J. Bowen, A. Bylinkin, J. Castle, S. Khalil, A. Kropivnitskaya, D. Majumder, W. Mcbrayer, M. Murray, C. Rogan, S. Sanders, E. Schmitz, J. D. Tapia Takaki, Q. Wang

Kansas State University, Manhattan, USA

S. Duric, A. Ivanov, K. Kaadze, D. Kim, Y. Maravin, D. R. Mendis, T. Mitchell, A. Modak, A. Mohammadi

Lawrence Livermore National Laboratory, Livermore, USA

F. Rebassoo, D. Wright

University of Maryland, College Park, USA

A. Baden, O. Baron, A. Belloni, S. C. Eno, Y. Feng, C. Ferraioli, N. J. Hadley, S. Jabeen, G. Y. Jeng, R. G. Kellogg, J. Kunkle, A. C. Mignerey, S. Nabili, F. Ricci-Tam, M. Seidel, Y. H. Shin, A. Skuja, S. C. Tonwar, K. Wong

Massachusetts Institute of Technology, Cambridge, USA

D. Abercrombie, B. Allen, V. Azzolini, A. Baty, R. Bi, S. Brandt, W. Busza, I. A. Cali, M. D'Alfonso, G. Gomez Ceballos, M. Goncharov, P. Harris, D. Hsu, M. Hu, Y. Iiyama, M. Klute, D. Kovalskyi, Y.-J. Lee, P. D. Luckey, B. Maier, A. C. Marini, C. Mcginn, C. Mironov, S. Narayanan, X. Niu, C. Paus, D. Rankin, C. Roland, G. Roland, Z. Shi, G. S. F. Stephans, K. Sumorok, K. Tatar, D. Velicanu, J. Wang, T. W. Wang, B. Wyslouch

University of Minnesota, Minneapolis, USA

A. C. Benvenuti[†], R. M. Chatterjee, A. Evans, P. Hansen, J. Hiltbrand, Sh. Jain, S. Kalafut, M. Krohn, Y. Kubota, Z. Lesko, J. Mans, R. Rusack, M. A. Wadud

University of Mississippi, Oxford, USA

J. G. Acosta, S. Oliveros

University of Nebraska-Lincoln, Lincoln, USA

E. Avdeeva, K. Bloom, D. R. Claes, C. Fangmeier, F. Golf, R. Gonzalez Suarez, R. Kamalieddin, I. Kravchenko, J. Monroy, J. E. Siado, G. R. Snow, B. Stieger

State University of New York at Buffalo, Buffalo, USA

A. Godshalk, C. Harrington, I. Iashvili, A. Kharchilava, C. Mclean, D. Nguyen, A. Parker, S. Rappoccio, B. Roozbahani

Northeastern University, Boston, USA

G. Alverson, E. Barberis, C. Freer, Y. Haddad, A. Hortiangtham, G. Madigan, D. M. Morse, T. Orimoto, A. Tishelman-charny, T. Wamorkar, B. Wang, A. Wisecarver, D. Wood

Northwestern University, Evanston, USA

S. Bhattacharya, J. Bueghly, O. Charaf, T. Gunter, K. A. Hahn, N. Odell, M. H. Schmitt, K. Sung, M. Trovato, M. Velasco

University of Notre Dame, Notre Dame, USA

R. Bucci, N. Dev, R. Goldouzian, M. Hildreth, K. Hurtado Anampa, C. Jessop, D. J. Karmgard, K. Lannon, W. Li, N. Loukas, N. Marinelli, F. Meng, C. Mueller, Y. Musienko[39], M. Planer, R. Ruchti, P. Siddireddy, G. Smith, S. Taroni, M. Wayne, A. Wightman, M. Wolf, A. Woodard

The Ohio State University, Columbus, USA

J. Alimena, L. Antonelli, B. Bylsma, L. S. Durkin, S. Flowers, B. Francis, C. Hill, W. Ji, T. Y. Ling, W. Luo, B. L. Winer

Princeton University, Princeton, USA

S. Cooperstein, G. Dezoort, P. Elmer, J. Hardenbrook, N. Haubrich, S. Higginbotham, A. Kalogeropoulos, S. Kwan, D. Lange, M. T. Lucchini, J. Luo, D. Marlow, K. Mei, I. Ojalvo, J. Olsen, C. Palmer, P. Piroué, J. Salfeld-Nebgen, D. Stickland, C. Tully

University of Puerto Rico, Mayagüez, USA

S. Malik, S. Norberg

Purdue University, West Lafayette, USA

A. Barker, V. E. Barnes, S. Das, L. Gutay, M. Jones, A. W. Jung, A. Khatiwada, B. Mahakud, D. H. Miller, N. Neumeister, C. C. Peng, S. Piperov, H. Qiu, J. F. Schulte, J. Sun, F. Wang, R. Xiao, W. Xie

Purdue University Northwest, Hammond, USA

T. Cheng, J. Dolen, N. Parashar

Rice University, Houston, USA

Z. Chen, K. M. Ecklund, S. Freed, F. J. M. Geurts, M. Kilpatrick, A. Kumar, W. Li, B. P. Padley, R. Redjimi, J. Roberts, J. Rorie, W. Shi, Z. Tu, A. Zhang

University of Rochester, Rochester, USA

A. Bodek, P. de Barbaro, R. Demina, Y. t. Duh, J. L. Dulemba, C. Fallon, T. Ferbel, M. Galanti, A. Garcia-Bellido, J. Han, O. Hindrichs, A. Khukhunaishvili, E. Ranken, P. Tan, R. Taus

Rutgers, The State University of New Jersey, Piscataway, USA

B. Chiarito, J. P. Chou, Y. Gershtein, E. Halkiadakis, A. Hart, M. Heindl, E. Hughes, S. Kaplan, R. Kunnawalkam Elayavalli, S. Kyriacou, I. Laflotte, A. Lath, R. Montalvo, K. Nash, M. Osherson, H. Saka, S. Salur, S. Schnetzer, D. Sheffield, S. Somalwar, R. Stone, S. Thomas, P. Thomassen

University of Tennessee, Knoxville, USA

H. Acharya, A. G. Delannoy, J. Heideman, G. Riley, S. Spanier

Texas A&M University, College Station, USA

O. Bouhali[73], A. Celik, M. Dalchenko, M. De Mattia, A. Delgado, S. Dildick, R. Eusebi, J. Gilmore, T. Huang, T. Kamon[74], S. Luo, D. Marley, R. Mueller, D. Overton, L. Pernie, D. Rathjens, A. Safonov

Texas Tech University, Lubbock, USA

N. Akchurin, J. Damgov, F. De Guio, P. R. Dudero, S. Kunori, K. Lamichhane, S. W. Lee, T. Mengke, S. Muthumuni, T. Peltola, S. Undleeb, I. Volobouev, Z. Wang, A. Whitbeck

Vanderbilt University, Nashville, USA

S. Greene, A. Gurrola, R. Janjam, W. Johns, C. Maguire, A. Melo, H. Ni, K. Padeken, F. Romeo, P. Sheldon, S. Tuo, J. Velkovska, M. Verweij, Q. Xu

University of Virginia, Charlottesville, USA

M. W. Arenton, P. Barria, B. Cox, R. Hirosky, M. Joyce, A. Ledovskoy, H. Li, C. Neu, T. Sinthuprasith, Y. Wang, E. Wolfe, F. Xia

Wayne State University, Detroit, USA

R. Harr, P. E. Karchin, N. Poudyal, J. Sturdy, P. Thapa, S. Zaleski

University of Wisconsin-Madison, Madison, WI, USA

J. Buchanan, C. Caillol, D. Carlsmith, S. Dasu, I. De Bruyn, L. Dodd, B. Gomber[75], M. Grothe, M. Herndon, A. Hervé, U. Hussain, P. Klabbers, A. Lanaro, K. Long, R. Loveless, T. Ruggles, A. Savin, V. Sharma, N. Smith, W. H. Smith, N. Woods

† **Deceased**

 1: Also at Vienna University of Technology, Vienna, Austria
 2: Also at IRFU, CEA, Université Paris-Saclay, Gif-sur-Yvette, France
 3: Also at Universidade Estadual de Campinas, Campinas, Brazil
 4: Also at Federal University of Rio Grande do Sul, Porto Alegre, Brazil
 5: Also at Université Libre de Bruxelles, Bruxelles, Belgium
 6: Also at University of Chinese Academy of Sciences, Beijing, China
 7: Also at Institute for Theoretical and Experimental Physics, Moscow, Russia
 8: Also at Joint Institute for Nuclear Research, Dubna, Russia
 9: Also at Cairo University, Cairo, Egypt
10: Also at Zewail City of Science and Technology, Zewail, Egypt
11: Also at British University in Egypt, Cairo, Egypt
12: Now at Ain Shams University, Cairo, Egypt
13: Also at Department of Physics, King Abdulaziz University, Jeddah, Saudi Arabia
14: Also at Université de Haute Alsace, Mulhouse, France
15: Also at Skobeltsyn Institute of Nuclear Physics, Lomonosov Moscow State University, Moscow, Russia
16: Also at Tbilisi State University, Tbilisi, Georgia
17: Also at CERN, European Organization for Nuclear Research, Geneva, Switzerland
18: Also at RWTH Aachen University, III. Physikalisches Institut A, Aachen, Germany
19: Also at University of Hamburg, Hamburg, Germany
20: Also at Brandenburg University of Technology, Cottbus, Germany
21: Also at Institute of Physics, University of Debrecen, Debrecen, Hungary
22: Also at Institute of Nuclear Research ATOMKI, Debrecen, Hungary
23: Also at MTA-ELTE Lendület CMS Particle and Nuclear Physics Group, Eötvös Loránd University, Budapest, Hungary
24: Also at Indian Institute of Technology Bhubaneswar, Bhubaneswar, India
25: Also at Institute of Physics, Bhubaneswar, India
26: Also at Shoolini University, Solan, India
27: Also at University of Visva-Bharati, Santiniketan, India
28: Also at Isfahan University of Technology, Isfahan, Iran
29: Also at Plasma Physics Research Center, Science and Research Branch, Islamic Azad University, Tehran, Iran
30: Also at Italian National Agency for New Technologies, Energy and Sustainable Economic Development, Bologna, Italy

31: Also at Università degli Studi di Siena, Siena, Italy

32: Also at Scuola Normale e Sezione dell'INFN, Pisa, Italy

33: Also at Kyung Hee University, Department of Physics, Seoul, Korea

34: Also at Riga Technical University, Riga, Latvia

35: Also at International Islamic University of Malaysia, Kuala Lumpur, Malaysia

36: Also at Malaysian Nuclear Agency, MOSTI, Kajang, Malaysia

37: Also at Consejo Nacional de Ciencia y Tecnología, Mexico City, Mexico

38: Also at Warsaw University of Technology, Institute of Electronic Systems, Warsaw, Poland

39: Also at Institute for Nuclear Research, Moscow, Russia

40: Now at National Research Nuclear University 'Moscow Engineering Physics Institute' (MEPhI), Moscow, Russia

41: Also at St. Petersburg State Polytechnical University, St. Petersburg, Russia

42: Also at University of Florida, Gainesville, USA

43: Also at P.N. Lebedev Physical Institute, Moscow, Russia

44: Also at California Institute of Technology, Pasadena, USA

45: Also at Budker Institute of Nuclear Physics, Novosibirsk, Russia

46: Also at Faculty of Physics, University of Belgrade, Belgrade, Serbia

47: Also at University of Belgrade, Belgrade, Serbia

48: Also at INFN Sezione di Pavia^a, Università di Pavia^b, Pavia, Italy

49: Also at National and Kapodistrian University of Athens, Athens, Greece

50: Also at Universität Zürich, Zurich, Switzerland

51: Also at Stefan Meyer Institute for Subatomic Physics (SMI), Vienna, Austria

52: Also at Adiyaman University, Adiyaman, Turkey

53: Also at Istanbul Aydin University, Istanbul, Turkey

54: Also at Mersin University, Mersin, Turkey

55: Also at Piri Reis University, Istanbul, Turkey

56: Also at Ozyegin University, Istanbul, Turkey

57: Also at Izmir Institute of Technology, Izmir, Turkey

58: Also at Marmara University, Istanbul, Turkey

59: Also at Kafkas University, Kars, Turkey

60: Also at Istanbul University, Istanbul, Turkey

61: Also at Istanbul Bilgi University, Istanbul, Turkey

62: Also at Hacettepe University, Ankara, Turkey

63: Also at Rutherford Appleton Laboratory, Didcot, United Kingdom

64: Also at School of Physics and Astronomy, University of Southampton, Southampton, United Kingdom

65: Also at Monash University, Faculty of Science, Clayton, Australia

66: Also at Bethel University, St. Paul, USA

67: Also at Karamanoğlu Mehmetbey University, Karaman, Turkey

68: Also at Purdue University, West Lafayette, USA

69: Also at Beykent University, Istanbul, Turkey

70: Also at Bingol University, Bingol, Turkey

71: Also at Sinop University, Sinop, Turkey

72: Also at Mimar Sinan University, Istanbul, Istanbul, Turkey

73: Also at Texas A&M University at Qatar, Doha, Qatar

74: Also at Kyungpook National University, Daegu, Korea

75: Also at University of Hyderabad, Hyderabad, India